

## THE *r*- AND *s*-PROCESS NUCLEI IN THE EARLY HISTORY OF THE GALAXY: HD 122563

CHRISTOPHER SNEDEN AND M. PARTHASARATHY

Department of Astronomy, University of Texas at Austin

Received 1982 July 26; accepted 1982 October 7

### ABSTRACT

New high-resolution, high signal-to-noise spectra in the blue and ultraviolet spectral regions have been obtained for the extremely metal-poor giant star HD 122563. A complete model atmosphere, spectrum synthesis analysis of this star has been performed, employing a large number of weak iron-peak species lines and laboratory oscillator strengths. Spectral features of many rare earth elements have been detected in the ultraviolet. The large overdeficiency of nearly a factor of 10 for the *s*-process element barium is confirmed and is shown to extend to the other *s*-process elements La, Ce, Pr, Nd, and Sm. The *r*-process elements Eu, Gd, Dy, and possibly Er and Yb are less deficient than the *s*-process elements but do exhibit lower ratios with respect to iron-peak elements than in the Sun. A supplementary differential analysis of HD 122563 with respect to the Sun shows that the heavy-element abundances are not very model-atmosphere dependent. The heavy-element abundances can be understood with nucleosynthesis models in which the progenitors of this star produce mainly *r*-process isotopes. A small contribution of the *s*-process to the creation of the elements Sr, Y, Zr, and possibly Ba is not ruled out, but such traditional *s*-process elements as La, Pr, and Nd appear to have been made in the *r*-process in stellar generations prior to the formation of HD 122563.

*Subject headings:* nucleosynthesis — stars: abundances — stars: atmospheres — stars: individual — stars: weak-line

### I. INTRODUCTION

Atomic nuclei generated by *s*(low) and *r*(apid) fluxes of neutrons carry important information about the very late stages of stellar evolution in the Galaxy. For example, detailed analyses of the elements primarily produced by the *s*-process have been used to help define the duration, frequency, and neutron sources of the thermal pulses of core and shell flash stars (e.g., see Sackmann, Smith, and Despain 1974; Cowley and Downs 1980; Tomkin and Lambert 1982). Investigations of the solar system abundances of elements produced mainly by the *r*-process have led theoreticians to conclude that classical supernovae are the most likely sites for *r*-process synthesis (e.g., see the review paper by Trimble 1975). Theoretical and observational difficulties in working with the *r*-process nuclei have prevented a more detailed description of their synthesis in highly evolved stars.

In this paper we begin a reexamination of the heavy-element synthesis in the early history of the Galaxy. Many heavy elements of the rare earth group and beyond possess more than one stable and abundant isotope; these isotopes in general are produced by the *r*- or *s*-process or both. Cameron (1982) has performed the most recent assignment of neutron capture processes for each isotope of the heavy elements in the solar system. Ideally we would like to have the same information on the abundance of all stable isotopes of each heavy

element for stars of interest. Since stellar atomic absorption spectra yield abundances only for a whole element, a definite assignment of an element to the *r*- or *s*-process is in general not possible. For this paper we will refer to *r*- and *s*-process elements as those whose most abundant isotopes in the solar system are produced by the appropriate synthesis process (Cameron 1982). It is recognized that such distinctions may not be appropriate for the isotopic mix of elements in another galactic epoch.

To first order the *r*-process nuclei are considered primary nucleosynthesis products of a star while the *s*-process nuclei are secondary. This means that a massive star which begins its life with zero metal content can in principle produce *r*-process rare earths such as Eu, Gd, Dy, etc. In particular these elements will be synthesized from iron-peak elements at the time that the star experiences its supernova explosion, and thus both the iron-peak and the *r*-process elements ought to be manufactured in reasonable amounts in each stellar generation. On the other hand, the *s*-process elements such as the Sr, Y, and Zr group and the Ba to Sm group are built through the slow neutron captures possible under quiescent stellar burning conditions. The iron-peak seed nuclei therefore must be present in the star prior to the late stages of its evolution, and normally would need to be produced in the preceding stellar generation. In this sense the *s*-process nuclei are secondary synthesis products, and their production might tend to lag behind

the synthesis of the iron peak and the  $r$ -process elements in the first generations of stars in the Galaxy.

The classic method of tracing the stellar nucleosynthesis sites of the early galactic generations is to compare the abundance pattern of extremely metal-poor stars to that of the Sun. This approach works well for ordinary metals, such as iron, which possess many very strong absorption lines in stellar spectra, but fails almost completely for the heavier rare earths. This is due mainly to the intrinsic weakness, relative to photographic plate grain noise, of transitions of neutral and ionized species of all heavy ( $Z > 40$ ) elements except Ba II. Moreover, the transitions of the rare earths detectable in most stellar spectra lie almost exclusively at wavelengths below 4500 Å, where the line crowding is severe. Systematic studies of large numbers of metal-poor stars therefore have had to rely primarily on only a couple of strong lines of Ba II to indicate the content of all heavy  $s$ -process elements (Peterson 1976; Luck and Bond 1981). Some attempts have been made to determine the content of La, Ce, and Nd from spectra of the brighter metal-poor stars (see, for example, Spite and Spite 1979), but generally the weakness of the spectral features and the use of intrinsically noisy photographic plate data have produced results which the various investigators themselves have not trusted.

Observational data are even more suspect for the  $r$ -process elements. In investigations of metal-poor stars, all abundance indicators for these elements usually have been reduced to one transition of Eu II at 4123 Å. Also, while Ba II lines retain appreciable strength even in the most metal-deficient cool star, the Eu II line is often quite difficult to identify, much less measure in very metal-poor stars. The most systematic investigation of  $r$ - and  $s$ -process element variations with overall stellar metallicity has been conducted by Butcher (1972, 1975). His study produced no compelling evidence for variations of the Eu/Fe abundance ratio, although his survey contained only two stars whose iron contents are less than  $[\text{Fe}/\text{H}] = -1.0$ .<sup>1</sup> Other investigators have reported europium abundances for some of the brighter very metal-poor stars, but the quoted errors are typically much larger than those for iron-peak elements or for barium. In Figure 1 we show Eu/Fe ratios from some earlier studies to illustrate the state of observational data on the  $r$ -process in metal-poor stars. Note in particular the large scatter from star to star, as well as the tendency toward large values of Eu/Fe in metal-poor stars. The scatter may be real or simply may be a reflection of the difficulties inherent in the derivation of Eu abundances.

The present study aims to supply reliable, more detailed abundances of the rare earth elements in metal-

<sup>1</sup>In this paper we adopt the standard spectroscopic notation  $[X] = \log_{10}(X)_{\text{star}} - \log_{10}(X)_{\text{sun}}$ , where  $X$  is any quantity.

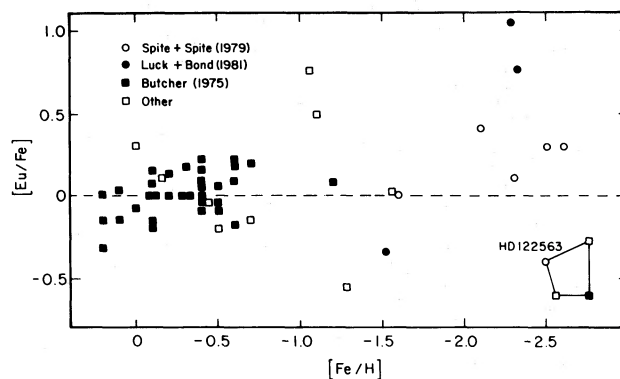


FIG. 1.—Some previous determinations of the Eu/Fe ratios in metal-poor stars. The Eu abundance determinations for HD 122563 of different investigators have been connected in the figure. Contributions for the open squares come from the studies of Koelbloed (1967), Tomkin (1972), Pagel (1964), Peterson (1976), and Mackle *et al.* (1975).

deficient stars. We seek first to discover whether Ba and Eu are accurate indicators of the whole of the  $r$ - and  $s$ -process element contents. Also we wish to address the problem of the apparent large scatter in the Eu abundances at a given metallicity, as well as the apparent trend toward large values of Eu/Fe in metal-poor stars. If the scatter is real, then Eu can prove to be an important probe of nucleosynthesis sites in the Galaxy and can provide constraints on the efficiency of mixing of the elements in early galactic generations. In this paper we report a detailed analysis of the brightest extremely metal-deficient star in the sky, HD 122563.

The star HD 122563 is one of the few stars in the Bright Star Catalog which possess metallicities less than  $[\text{Fe}/\text{H}] = -1$ ; as such, its spectrum has been analysed several times. Wallerstein *et al.* (1963) obtained the original high-resolution spectroscopic plate data and derived  $[\text{Fe}/\text{H}] = -2.7$  from a coarse analysis of the spectrum of this star. Using the same line data set, Pagel's (1965) coarse analysis yielded  $[\text{Fe}/\text{H}] = -2.55$ , while Wolfram's (1972) model atmosphere fine analysis gave  $[\text{Fe}/\text{H}] = -2.75$ . Wolff and Wallerstein (1967) made the first attempt to use ultraviolet spectra for abundance studies in HD 122563. They derived abundance ratios of iron-peak elements with respect to iron, but no absolute metallicity for this star was determined. However, the abundance ratios from their ultraviolet spectra showed encouraging agreement with those of Pagel's (1965) analysis of the original blue-visual spectra. More recent abundance determinations for HD 122563, employing model atmosphere analyses and independent line data sets, include those of Spite and Spite (1979) and Luck and Bond (1981); all metallicity determinations now agree at  $[\text{Fe}/\text{H}] = -2.65 \pm 0.2$ .

Several of the studies of HD 122563 also have derived large overdeficiencies of Ba and a possible overde-

iciency of Eu. The CNO group of elements in this star have been shown to exhibit nonsolar abundance ratios: enhanced nitrogen and depleted carbon (Snedden 1973), overabundant oxygen (Lambert, Sneden, and Ries 1974), and an abnormally low carbon isotope ratio (Lambert and Sneden 1977). These light-element abundances, coupled with the high luminosity of HD 122563, clearly indicate a star in an advanced evolutionary state.

In § II of this paper we present new observational data of high-resolution and high signal-to-noise in the blue and ultraviolet spectral regions of HD 122563. In § III we discuss the model atmosphere analysis of HD 122563 using laboratory oscillator strengths, as well as a differential analysis with respect to the Sun. In § IV we show the derivation of all element abundances, and in § V we discuss the implications of our results for galactic nucleosynthesis.

## II. OBSERVATIONS AND REDUCTIONS

New spectroscopic observations of HD 122563 were obtained with the McDonald Observatory 2.7 m telescope and coudé spectrograph. For blue and ultraviolet spectra the Digicon silicon diode array (Tull, Choisser, and Snow 1975) was employed as the detector. This spectrograph-detector combination provided digital spectra with 2-diode resolutions of approximately 0.13 Å, wavelength coverage of about 55 Å, and signal-to-noise values of, usually, about 100. For spectra at longer wavelengths than 5000 Å we used a Reticon silicon diode array (Vogt, Tull, and Kelton 1978). This instrument produced spectra with 2-diode resolutions of 0.20 Å, wavelength ranges of 90 Å, and signal-to-noise ratios greater than 200. The higher signal-to-noise values for the Reticon spectra were possible due to a combination of the lower resolution of the Reticon spectra and the much larger intrinsic flux for the K-giant program star at longer wavelengths. Integration times for these spectra ranged from 3/4 hour to about 4 hours. We obtained nearly continuous spectral coverage from 3650 Å to 4700 Å and concentrated on the more promising spectral features in the wavelength ranges 3400–3650 Å and 4700–6500 Å. All spectra were flat-field corrected via division by lamp spectra, and the red spectra of the star were divided by spectra of featureless hot stars to remove terrestrial absorption lines.

We measured equivalent widths of all unblended atomic lines appearing on our spectra of HD 122563, approximating the line profiles with Gaussians. In general, continuum placement on the spectra was not difficult, due to the high signal-to-noise values of the spectra and the extreme metal deficiency of this star. Lines of less than 10 mÅ could be identified and measured on our spectra. The resulting line data set is given in Table 6 in the Appendix. This table also contains Gaussian measurements of the same features in the solar

spectrum in regions for which line crowding is not too severe. The source for the solar spectrum was the center-of-disk Liège Atlas (Delbouille, Neven, and Roland 1973). This atlas currently has wavelength coverage down to 3600 Å. We did not attempt to include solar line measurements from the older Utrecht Atlas (Minnaert, Mulders, and Houtgast 1940); the benefits of more solar line data would not outweigh the disadvantages of the lower signal-to-noise and small plot scale of that atlas. Note that the Gaussian approximation for line profiles is valid only for lines without very strong contributions from the wings ( $W_\lambda < 125$  mÅ). The entries in Table 6 show that all but a few lines in HD 122563 are well represented by the Gaussians. About 14% of the solar lines are stronger than 125 mÅ; however, the vast majority of these strongest lines were eliminated for the abundance analysis of HD 122563 relative to the Sun. Therefore the use of Gaussian line profile approximations introduced no significant errors in our abundances.

It is of course very difficult to analyze the blue-ultraviolet spectra of stars whose spectral types are cooler than F. The massive line blocking below 4000 Å characteristic of these stars, however, is not an extreme problem for the very metal-poor star HD 122563. A comparison of our spectra with that of the Liège atlas suggests that, if atomic parameters are available for relevant absorption features, HD 122563 may be analyzed more easily than the Sun in the blue-ultraviolet wavelength regions.

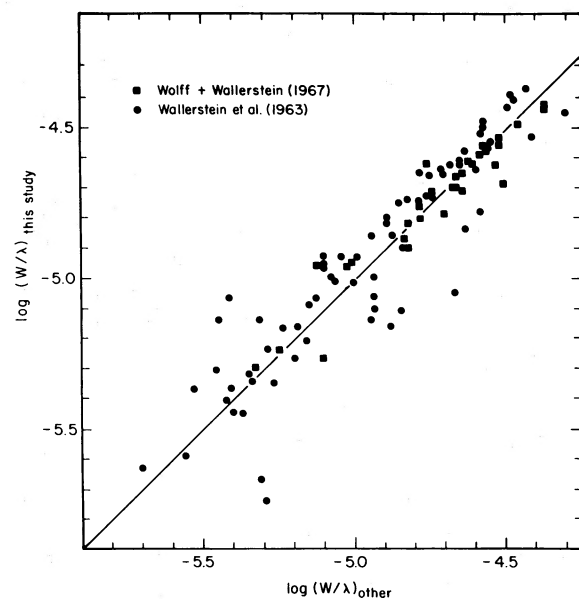


FIG. 2.—A comparison of the equivalent widths of this study with those of two previous high-resolution analyses. The straight line defines equality between the measurements.

In Figure 2 we compare the equivalent width scale of the present digital spectra with the scales of Wallerstein *et al.* (1963) and Wolff and Wallerstein (1967). No systematic differences exist between the equivalent width sets. The increase in scatter about the mean line for weak features is attributed mainly to the influence of plate grain noise on the measurement of weak-line equivalent widths from photographic spectra.

### III. MODEL ATMOSPHERE DERIVATION

Before discussing the heavy elements in HD 122563, we describe in this section a new determination of its model atmosphere parameters. Investigators have previously derived model atmospheres for the star, but several factors made a new attempt attractive. First, it is obvious from Table 6 that the line data available for HD 122563 has been expanded: for Fe I there are representative line measures at great ranges of excitation potential and equivalent width, and for the iron-peak elements in general there are five elements with line data for two species. These spectral features should be quite sensitive to model atmosphere parameter variations. Second, within the past few years the accuracy and number of laboratory oscillator strengths has increased considerably. Almost invariably the improvement in oscillator strengths for a given species has led to closer agreement between that element abundance in the Sun and in meteorites. Stellar spectroscopy may not be far from the time when differential analyses of stars with respect to the Sun may be unnecessary. Third, the temperature scale for red giant stars has come under renewed scrutiny: Lambert and Ries (1981) and Ries (1982) have derived spectroscopic temperatures for early K giants which are systematically 150–300 K hotter than those derived from the standard Johnson (1966) temperature scale. Other investigators suggest that spectroscopic temperatures may be inappropriate for K giant stars: Ruland *et al.* (1980) claim that the low-lying excitation states of neutral atoms in the atmosphere of Pollux are significantly depopulated by radiation, and therefore are useless for the derivation of excitation temperatures. A final significant problem may be that a comparison of the spectrum of a red giant to that of the Sun stretches the differential abundance technique to unacceptable limits. For our analysis, for instance, the large differences seen between the ultraviolet spectra of the Sun and HD 122563 diminish the usefulness of a differential technique for some spectral features. With these problems and new possibilities at hand we chose to analyze HD 122563 with both laboratory oscillator strengths and “astrophysical” oscillator strengths derived through a differential analysis with respect to the Sun. The term *differential analysis* here is used to denote not the traditional single-slab, curve-of-growth method but rather the use of a standard solar model atmosphere,

solar abundances, and solar equivalent widths to derive a set of “astrophysical” oscillator strengths which then were applied to the spectrum of HD 122563. The accuracies of such *gf*-values are limited by the accuracies of the solar quantities, and to this extent the stellar analysis became a differential one.

We determined the atmosphere parameters for our star with a standard curve-of-growth, model atmosphere technique. Stellar model atmospheres were obtained from the red giant atmosphere grid of Bell *et al.* (1976), using the interpolation routines of P. L. Cottrell (1982, private communication). Oscillator strengths were taken from the literature; our choices of these parameters are discussed in the Appendix. We employed the LTE line analysis and spectrum synthesis routines described by Sneden (1973); these routines produce spectrum profiles and equivalent widths of spectral features from input consisting of a model atmosphere, assumed metal abundances, and atomic and/or molecular line parameters. The input model atmospheres were altered until the following standard criteria were satisfied. We first looked for equality of abundances for lines of given species with (a) low and high excitation potentials, (b) small and large equivalent widths, and (c) very large differences in wavelength. These criteria determined values of  $T_{\text{eff}}$  and microturbulent velocity, and provided checks on our continuum placements and continuous opacity sources as functions of wavelength. We set gravities for the models through the balance of abundances from neutral and ionized species of all possible elements. Note that gravities determined through ionization equilibrium inevitably are somewhat dependent on adopted  $T_{\text{eff}}$  parameters; a choice of higher  $T_{\text{eff}}$  forces a higher gravity to maintain equilibrium between neutral and ionized species.

In the spectrum of HD 122563 there were enough Fe I absorption features to perform all tests mentioned above, and the rest of the iron-peak elements provided features to refine the gravity estimate for this star. With our line data, it was not possible to satisfy completely all atmosphere criteria with a single stellar model. For instance, to produce no trend of Fe I abundances with line excitation potentials, trial models with  $T_{\text{eff}} = 4450$  K were adopted initially. However, use of these low temperature models yielded severe trends of Fe I abundances with wavelength: abundances from ultraviolet lines were larger than those from yellow-red lines by almost a factor of 10. This problem arose from the balance of  $\text{H}^-$  and H-Rayleigh scattering continuous opacities in the atmosphere of HD 122563. For giant stars of very low metallicity, the Rayleigh scattering is a significant opacity source and dominates in the ultraviolet. This scattering is virtually temperature independent while  $\text{H}^-$  has a severe temperature dependency through large changes in atmosphere electron densities with metal ionization changes. Therefore our initial

atmosphere choice of  $T_{\text{eff}} = 4450$  K produced continuous opacities at long wavelengths (largely from  $\text{H}^-$ ) which were too low with respect to those at short wavelengths (from Rayleigh scattering), and hence brought about the apparent overabundances of ultraviolet Fe I lines. This result was anticipated by Wolff and Wallerstein (1967), who derived ratios of  $\text{H}^-$  to Rayleigh opacities from the evidence of their line data for HD 122563. Their result, that the continuous opacities must be adjusted to yield line strengths  $\log(W/\lambda)$  essentially independent of wavelength, was confirmed in our analysis. However, the cross sections for these continuous opacity sources are now well established (see the references in Kurucz 1970), and all adjustments of the total opacities must be done with alteration of the model atmosphere physical parameters. In particular, raising  $T_{\text{eff}}$  values by about 100 K increased the number of  $\text{H}^-$  absorbers, raised the long wavelength continuous opacities, and provided the desired wavelength-independent Fe I abundances. Through consideration of such links between the iron-peak line abundances and atmosphere parameters, we iterated to a final model for HD 122563.

In Figure 3 we show the trends of Fe I abundances for the best compromise model,  $(T_{\text{eff}}/\log g/[M/H]/v_{\text{micro}}) = (4525 \text{ K}/0.60/-2.5/2.3 \text{ km s}^{-1})$ . Remaining trends are not large; note in particular that model parameters  $T_{\text{eff}}$ ,  $\log g$ , and  $[M/H]$  do not depend strongly on the adopted value of the microturbulent velocity, for at least half of the iron-peak lines in HD 122563 are weaker than  $\log(W/\lambda) = -5.0$  and thus are largely unsaturated. A few species other than Fe I show lines with a broad range in excitation potential. Inspection of the abundance trends for these species revealed good agreement with the Fe I results. In Table 1 we compare the derived model parameters from this and other analyses. The use of an analysis with laboratory *gf*-values has resulted in a lower effective temperature for HD 122563 than has been derived by other, differential analyses. The temperature estimate from this study is, however, within the stated errors of earlier temperature estimates. The lower effective temperature automatically yields a lower gravity estimate here, but again this parameter is not very different than those derived by Spite and Spite (1979) and Luck and Bond (1981). The microturbulence from our analysis disagrees with the determination of Luck and Bond (1981), but the line data of those authors did not contain enough very weak Fe I lines to determine this quantity accurately. Finally, our iron abundance is in excellent agreement with all recent analyses.

How reliable is this new, somewhat lower temperature? The broad-band *UBVRI* colors of HD 122563 have been discussed by Spite and Spite (1979), who gave intrinsic Johnson system colors of  $B - V = 0.90$  and  $R - I = 0.59$ , and suggested that no reddening corrections were needed for this nearby giant. Bond (1980)

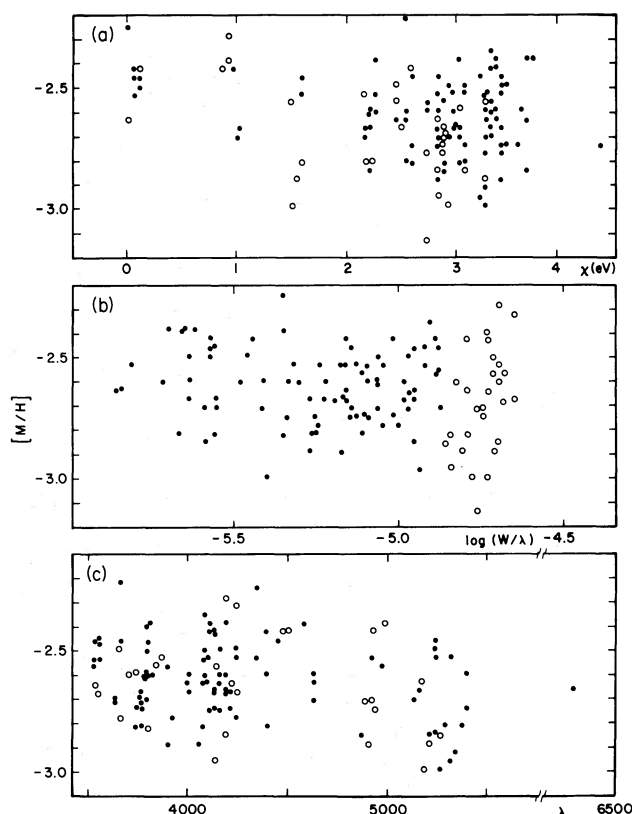


FIG. 3.—Trends of Fe I abundances with (a) excitation potentials, (b) equivalent widths, and (c) wavelengths of the lines. The filled circles represent lines with strengths less than  $\log(W/\lambda) = -4.85$ , and open circles represent stronger lines.

measured Strömgen *uvby* intermediate-band colors for this star, and reported a value of 0.640 for the temperature-sensitive  $b - y$  index. The  $B - V$  and  $b - y$  indices both indicate a temperature from 4600 K to 4750 K, using any of the Johnson (1966), Bell and Gustafsson (1978), or Cohen, Frogel, and Persson (1978) effective temperature calibrations. (The  $T_{\text{eff}}$  versus  $b - y$  relationship of Luck and Bond 1981 provides no independent check here, for HD 122563 was one of the stars used to define their relationship.) However, the temperature calibrations of Bell and Gustafsson (1978) and Cohen, Frogel, and Persson (1978), which were carried out for a variety of atmosphere parameters, demonstrate that the colors from ultraviolet to visual wavelengths are extremely sensitive to model gravity in the K giant domain. Typically, changes of 0.04 to 0.11 in the colors are seen for changes of 0.5 in  $\log(g)$ . Also, at the extreme metal deficiency characteristic of HD 122563 the short-wavelength colors show smaller but not negligible variations with metallicity changes. On the other hand, the  $(R - I)$  versus  $T_{\text{eff}}$  color calibration derived by Cohen, Frogel, and Persson (1978) is much less sensitive to

TABLE 1  
MODEL ATMOSPHERE PARAMETERS FOR HD 122563

$T_{\text{eff}}$ (K)	$\log g$	$v_t$	[Fe/H]	Source
$4600 \pm 150 \dots$	$1.2 \pm 0.4$	$2.6 \pm 0.4$	$-2.75 \pm 0.3$	Wolfram 1972
$4580 \pm 100 \dots$	0.9	1.8	-2.5	Spite and Spite 1979
$4600 \pm 200 \dots$	$0.8 \pm 0.3$	$3.2 \pm 0.5$	$-2.59 \pm 0.2$	Luck and Bond 1981
$4525 \pm 150 \dots$	$0.6 \pm 0.4$	$2.3 \pm 0.4$	$-2.65 \pm 0.2$	lab $gf$ -values
$4700 \pm 150 \dots$	$1.4 \pm 0.4$	$2.3 \pm 0.4$	$-2.40 \pm 0.2$	solar $gf$ -values

gravity and metallicity: even for cool, low-gravity stars, large changes in  $\log(g)$  and [Fe/H] produce changes of only 0.01–0.02 in  $R - I$ . We therefore chose the  $R - I$  color as primary photometric  $T_{\text{eff}}$  index. This color index for HD 122563 implies an effective temperature of 4460 K with the Johnson (1966) calibration and about 4450 K with the Cohen, Frogel, and Persson (1978) scale. These values, of course, clearly support a temperature lower than 4600 K for this star, in agreement with our purely spectroscopic temperature determination.

Additional atmosphere information comes from the spectrum of HD 122563 below 3000 Å. Gustafsson *et al.* (1980) studied the ultraviolet flux of this star with the *IUE* satellite. They showed that the observed flux in the region from 2300 Å to 2800 Å could be matched well with a standard model atmosphere with parameters (4600/1.20/−2.70/2). Increasing the model gravity to  $\log g = 1.70$  produced fluxes too large to match the observed spectrum, while a decrease in temperature to  $T_{\text{eff}} = 4500$  K naturally yielded smaller ultraviolet fluxes than demanded by the observations. Therefore, if our derived (4525/0.60/−2.50/2.3) model is correct, then HD 122563 is anomalously bright in the ultraviolet compared to the theoretical models. This follows the trend of the *U* and *B* broad-band colors and can indicate either inadequacies in the theoretical models or incorrect derived  $T_{\text{eff}}$  and/or  $\log g$  parameters for those models.

A differential curve-of-growth, model atmosphere analysis with respect to the Sun was carried out using the solar line measures given in Table 6 and the empirical solar model atmosphere of Holweger and Müller (1974). This solar model is preferred by many workers in solar spectroscopy; a discussion of the relative merits of various solar models for abundance studies is given in Lambert (1978) and will not be repeated here. Note here, however, that derived solar Fe I oscillator strengths for weak lines used in our study showed reasonable agreement with the lab  $gf$ 's of these lines determined by the Blackwell group. We adopted a depth-independent value of  $0.8 \text{ km s}^{-1}$  for the solar microturbulence, and employed standard van der Waals line damping formulae with the modification to the damping constant suggested by Holweger (1971). While introducing solar

atmosphere uncertainties into the abundance determination, the differential approach tends to cancel scale and scatter problems in the oscillator strengths. Indeed, plots similar to those of Figure 3 for the differential analysis showed the scatter of Fe I abundances from individual lines reduced by about 0.2 from that of the absolute analysis. We iterated on model atmosphere parameters for HD 122563 with respect to the solar model until the same criteria discussed for the absolute analysis were satisfied. Final model atmosphere parameters are listed in Table 1; obviously the differential analysis gave much higher values for  $T_{\text{eff}}$  and  $\log(g)$  than the absolute- $gf$  approach. Note, however, the overall relative insensitivity of the microturbulence and [Fe/H] to the temperature and gravity changes. Finally, the two models determined in this study probably define the extreme ranges permitted for the atmosphere parameters of HD 122563 and as such provide constraints on the element abundance ratios in this star.

The clash of model atmosphere parameters from the two analysis methods may have relevance to the red giant temperature scale discussion. Departures from LTE in red giant atmospheres may be expected to produce an overionization of neutral species, and also a depopulation of the lowest excitation levels of at least the neutral species. If non-LTE effects are present in the atmosphere but not properly accounted for, the stellar model resulting from an LTE analysis will be too hot (low level depopulation) and may have too low a gravity (overionization). However, from the absolute analysis of the spectrum of HD 122563 we derived a lower value of  $T_{\text{eff}}$  than is suggested from all differential analyses; this temperature also was lower than or comparable to that resulting from an analysis of the star's colors. This argues that no depopulation of low-excitation-potential states of the neutral species is occurring in HD 122563. No definitive statement may be made for the overionization effect; our lower derived gravity is consistent with the change needed by the lower  $T_{\text{eff}}$ . Note, however, that the gravity implied by the species balance for Fe (ionization potential = 7.87 eV) is slightly larger than that suggested by Ti (6.82 eV) or V (6.74 eV). Non-LTE overionization should affect the lower ionization potential element more, and this effect possibly may be pre-

sent in HD 122563. This same effect also could be due to remaining scatter and oscillator strength scale uncertainties, so the small ionization differences seen here are not reliable tests.

The large difference seen in the analysis with respect to the Sun strongly suggests, however, that part of the temperature scale uncertainty comes simply from the comparison of K giant radiative equilibrium model stellar atmospheres to the mostly empirical models of the G dwarf Sun. Sneden, Lambert, and Pilachowski (1981) previously have pointed out that use of solar model atmospheres other than the Holweger and Müller (1974) model can decrease the implied K giant temperatures by up to 100 K. Also, the opacity and temperature structure differences between stellar and solar atmospheres may as yet not be properly accounted for; a reinvestigation of the use of differential analyses with a solar standard in stellar abundance work may be necessary. As shown in the next section, the uncertainties due to analysis method apparently do not greatly affect the derived abundance pattern in HD 122563. A final caution on the application of our results to the red giant temperature scale question: the very large metal deficiency of HD 122563 produces a far different atmosphere structure from that for a Population I giant. A comparison of two models in the Bell *et al.* (1976) grid, both with  $T_{\text{eff}} = 4500$  and  $\log(g) = 0.75$ , but one with  $[\text{Fe}/\text{H}] = 0.0$  and one with  $[\text{Fe}/\text{H}] = -3.0$ , shows that the extremely metal-poor star has the same  $T(\tau)$  relation in the line-forming regions as its metal-rich companion. However, at identical optical depths the metal-poor star has nearly a factor of 10 greater  $P_g$  and a factor of 10 less  $P_e$ . Conclusions drawn from analyses of extremely metal-deficient objects may not apply directly to metal-rich stars.

#### IV. DETERMINATION OF THE RELATIVE ABUNDANCES

A straightforward analysis of the line data in Table 6 and the two models for HD 122563 gave the abundances of all other elements from Na through Ba. These abundances are listed in Table 2 along with the number of transitions actually used in the abundance derivations (some very strong lines and some lines which gave obviously discordant results were eliminated from the final sample). The excellent consistency of the abundance deficiencies for most iron-peak elements suggests that the overall metal content of HD 122563 has been established well. Our results are generally in fair accord with those of Spite and Spite (1979) which are listed in Table 2, and also agree well with the determinations of Wolfram (1972) and Luck and Bond (1981).

Special procedures were employed for a few of the iron-peak elements. Many lines of the elements Sc, V, and Co exhibit pronounced hyperfine structure (hfs) splitting. This splitting, which appears obvious on the

Liège solar atlas, in effect desaturates the lines and alters, often by large factors, the implied abundances for these elements. Since the abundances of Sc, V, and Co are of secondary interest for the present paper, we did not attempt to synthesize all of the (hfs) components for each line of these elements; moreover, the laboratory hfs data are lacking for many of the relevant transitions. To approximate the hfs splitting, we measured the full widths at half-maxima for our features in the solar spectrum, when they were available and unblended on the Liège atlas. The line breadths were converted to additional components of the turbulent velocity parameters for these species. The hfs velocity components ranged from 0.8 to 3.1 km s<sup>-1</sup>. Since hfs splitting cannot alter the equivalent width of a line which already is desaturated, the corrections generally proved to be smaller for the features of HD 122563 than for those of the Sun. Therefore the absolute analysis of these elements in our star provided more accurate abundances for these elements than did the differential procedure. Also, the hfs correction factors were far smaller for Sc and V than for Co, whose spectral features used in the absolute *gf* analysis were the strongest of the three elements. Caution should be exercised in the interpretation of the Co abundance listed in Table 2. Finally, Mn also exhibits hfs in its principal lines; however, those lines (e.g., the triplet of Mn I lines near 4030 Å) were not employed in our analysis, and lines used in this study are extremely weak in HD 122563. No hyperfine structure computations were employed for the Mn I lines.

The derivation of a Cr abundance also required special attention. As discussed in the Appendix, use of the best available oscillator strengths for the neutral and ionized species of this element leads to discordant abundances in the Sun. The solar Cr II lines indicate an abundance 0.57 dex larger than that derived from Cr I features. Moreover, use of the *gf*-values of Kurucz and Peytremann (1975) for both neutral and ionized species still leaves a 0.21 dex discrepancy between the abundances from these species. We chose to adopt a single value of the Cr abundance in the Sun,  $\log \epsilon = 5.7$  (Biémont 1976), and ignored Cr in the derivation of a gravity for HD 122563. The differential analysis of the star with respect to the Sun should remove this source of uncertainty but the entries in Table 2 show a remaining discrepancy between Cr I and Cr II. That disagreement could be lessened with the choice of a higher value of  $T_{\text{eff}}$  for HD 122563 in the differential analysis, but the data from other elements constrain the temperature to not much greater than 4700 K.

We have mentioned previously in this paper that the analysis of the rare earth elements was complicated by (a) their general weakness in HD 122563, (b) the appearance of their transitions in the ultraviolet spectral regions, and (c) the pronounced hfs broadening for at

TABLE 2  
 ABUNDANCES IN HD 122563

Species	log $\epsilon$ (Sun)	Source	[M/H] (Spite)	[M/H] <sup>a</sup>	[M/Fe] <sup>a</sup>	Lines <sup>a</sup>	[M/H] <sup>b</sup>	[M/Fe] <sup>b</sup>	Lines <sup>b</sup>
Na I.....	6.28	1	-2.3	-1.9::	+0.7::	1	-1.8::	+0.6::	1
Mg I.....	7.62	1	-2.4	-2.3::	+0.3::	2	-2.38	+0.02	1
Ca I.....	6.34	1	-2.4	-2.29	+0.36	13	-2.08	+0.32	8
Sc I.....	3.08	2	...	-2.61	+0.04	2	-2.47	-0.07	2
Sc II.....	3.08	2	-2.6	-2.66	-0.01	5	-2.46	-0.06	5
Ti I.....	4.98	3	-2.3	-2.44	+0.21	16	-2.36	+0.04	11
Ti II.....	4.98	3	-2.4	-2.38	+0.27	23	-2.35	+0.04	22
V I.....	4.14	2	-2.3	-2.68	-0.03	7	-2.58	-0.18	5
V II.....	4.14	2	...	-2.56	+0.09	12	-2.41	-0.01	5
Cr I.....	5.7:	4	-2.5	-2.7::	-0.1::	13	-2.92	-0.52	10
Cr II.....	5.7:	2	-2.3	-2.6::	+0.0::	5	-2.56	-0.16	4
Mn I.....	5.4:	2	-2.5	-2.9:	-0.3:	2	-2.9:	-0.5:	1
Fe I.....	7.58	5	-2.5	-2.61	+0.04	138	-2.33	+0.07	98
Fe II.....	7.58	5	-2.4	-2.66	-0.01	21	-2.45	-0.05	16
Co I.....	4.92	6	-2.3:	-2.4:	+0.2::	8	-2.2::	+0.2::	6
Ni I.....	6.29	7	-2.4	-2.74	-0.09	9	-2.48	-0.08	11
Sr II.....	2.90	8	...	-2.75	-0.10	2	...	...	...
Y II.....	2.24	9	-2.8	-3.08	-0.43	9	-2.79	-0.39	5
Zr II.....	2.56	10	-2.1:	-2.45:	+0.20:	6	-2.37:	+0.03:	3
Ba II.....	2.09	8	-3.2	-3.54	-0.89	5	-3.48	-1.08	5
La II.....	1.13	11	-2.0::	-3.35:	-0.70:	5	-3.28:	-0.88:	5
Ce II.....	1.55	11	-2.6::	< -3.0	< -0.4	3	< 2.9	< -0.5	3
Pr II.....	0.99	11	-3.0::	-3.3::	-0.7::	3	-3.2::	-0.8::	3
Nd II.....	1.26	12	-3.0::	-3.2::	-0.6::	3	-3.1::	-0.7::	3
Sm II.....	0.80	13	...	< -3.2	< -0.6	1	< 2.9	< -0.5	1
Eu II.....	0.51	14	-2.9:	-3.00	-0.35	5	-2.80	-0.40	5
Gd II.....	1.12	8	...	-3.15:	-0.50:	2	-3.05:	-0.65:	2
Dy II.....	1.06	8	...	-3.00	-0.35	4	-2.90	-0.40	4
Er II.....	0.76	8	...	-2.9::	-0.3::	2	-2.8::	-0.4::	2
Yb II.....	0.9	8	...	-3.0::	-0.4::	1	-2.9::	-0.5::	1

<sup>a</sup>Laboratory *gf* model.<sup>b</sup>Solar *gf* model.

REFERENCES FOR TABLE 2.—(1) Lambert and Luck 1978. (2) Biémont 1978. (3) Whaling, Scalo, and Testerman 1977. (4) Bieniewski 1976. (5) Aller 1980, private communication; best estimate from all recent studies. (6) Cardon *et al.* 1982. (7) Lennard *et al.* 1975. (8) Ross and Aller 1976. (9) Hannaford *et al.* 1982. (10) Biémont *et al.* 1981. (11) Andersen *et al.* 1975. (12) Maier and Whaling 1977. (13) Saffman and Whaling 1979. (14) Biémont *et al.* 1982.

least La and Eu. For these reasons we chose to analyze most of the rare-earth element lines with a spectrum synthesis technique. The only exceptions were Ba II, whose lines are still strong in HD 122563, and one line of La II for which an equivalent width could be measured with confidence.

Line selection is extremely important in the analysis of species which possess large numbers of transitions, all of which are extremely weak in the observed stellar spectrum. Indeed, some earlier abundance determinations of the *s*-process elements in HD 122563 have probably misidentified noise features as actual stellar absorption lines, and by that have derived too large abundances for those species. Our line identification effort relied on three primary sources: the compilation of solar absorption features of Moore, Minnaert, and Houtgast (1966), the list of laboratory spectral line intensities of Meggers, Corliss, and Scribner (1975), and

the tables of semiempirical *gf*-values by Kurucz and Peytremann (1975). We limited our transition search to only the leading lines of a species, that is, to those lines with large intensities in the lab (Meggers, Corliss, and Scribner 1975). Next we eliminated those lines which possess small equivalent widths (usually less than 20 mÅ) in the Sun; spot checks of these weak lines in the spectrum of HD 122563 revealed little hint of their presence in the star. Finally, lines that were severely blended in the solar spectrum or expected to be in the spectrum of HD 122563 were discarded. Here the tables of Kurucz and Peytremann (1975) proved especially valuable, often suggesting contaminating features which were not indicated in the solar spectrum.

As one example of the difficulties of rare-earth element line selection in the ultraviolet, consider the three lines attributed to Gd II near 3439 Å. Relevant parameters for these lines and those employed for our Gd

TABLE 3  
GADOLINIUM II LINE DATA

Wavelength	E.P. (eV)	$W_{\lambda}$ (Sun) (mÅ)	Emission Intensity	$\log(gf)$
3439.23 .....	0.38	10	1700	+0.04
3439.78 .....	0.42	66	830	-0.22
3439.99 .....	0.24	7.5	2700	+0.12
3549.36 .....	0.24	26	3900	+0.20
3768.39 .....	0.08	22	8700	+0.25

abundance derivation are given in Table 3. Solar equivalent widths are taken from Moore, Minnaert, and Houtgast (1966), emission intensities from Meggers, Corliss, and Scribner (1975), and oscillator strengths from Corliss and Bozman (1962). The solar feature at 3439.8 Å is by far the strongest line identified as Gd II in the solar spectrum longward of 3300 Å. However, its solar equivalent width is very inconsistent with its atomic parameters and with those of the neighboring Gd II lines. Solar and laboratory parameters for the other 3439 Å lines agree roughly with those expected from the much stronger 3549 Å and 3768 Å lines. In the spectrum of HD 122563, the two longer wavelength features were weak, and, as expected, no positive identification of the 3439.2 Å and 3440.0 Å lines was possible. A reasonably strong feature near 3439.8 Å was evident in the spectrum, but its measured wavelength was 3439.88 Å, a full 0.1 Å redward of the desired Gd II feature. Such a wavelength mismatch between stellar and laboratory transitions was unacceptably large. We therefore concluded that the promising 3439.8 Å Gd II feature was due to some other species and rejected it from our sample. The lines at 3549 Å and 3768 Å finally selected for our analysis were the only features of the 20 strongest transitions of Gd II listed by Meggers, Corliss, and Scribner (1975) which were reasonably unblended in solar and stellar spectra.

A comparison of the rare earth line lists of Wallerstein *et al.* (1963) and Spite and Spite (1979) with the present choice of lines reveals only two lines of Eu II in common. Of the two lines, only the 4129 Å feature yields a reliable abundance without spectrum synthesis; Pagel (1965) correctly put low weight on the 4205 Å line. For Ce II, Wallerstein *et al.* measured the 4186 Å line, while Spite and Spite (1979) attempted to use the 4349 Å feature. The 4186 Å line is one of the strongest transitions of Ce II, but unfortunately it is severely blended in the Sun and in HD 122563 by a CH line; inspection of our stellar spectrum suggests that most if not all of the absorption at 4186 Å is due to CH. The solar equivalent width of the 4349 Å line is 7.5 mÅ (Moore, Minnaert and Houtgast 1966), and this line is not identifiable on our spectra of HD 122563. Of the other rare earth features reported by Spite and Spite

(1979), only the Nd II line at 4358 Å has appreciable strength in the Sun: 38 mÅ. Once again it must be stressed that these earlier investigators put low weight on their line measures of the rare earth elements, and Spite and Spite (1979) in particular were prevented from seeking stronger rare earth lines by the limits of the wavelength coverage of their spectra. A comparable very low weight abundance determination in the present work is the case of Sm II: it exhibits one blended feature at 3568 Å which may be present in HD 122563; we have merely quoted an upper limit to its abundance. All other possible transitions of this element have not been detected in our spectra.

Line lists for the synthetic spectra were culled from the compendium of transitions of Kurucz and Peytremann (1975); neutral and ionized species lines with lower excitation potentials less than 4.5 eV were included in the lists. The lines of the CH molecule were added to these lists; the parameters for CH are discussed by Lambert (1978). We neglected the CN molecule because it is apparent in the spectrum of HD 122563 only at the (0-0) band head at 3883 Å (see Fig. 4 in Sneden 1973). Its extreme weakness, of course, is caused by its squared dependency on the metallicity of the star. Initially, we synthesized regions of the spectrum of HD 122563 using laboratory oscillator strengths where possible (see the references for Table 6); otherwise the Kurucz and Peytremann (1975) values were used. When possible, synthetic spectra were generated only for those lines of rare earth species for which modern laboratory oscillator strengths were available. As detailed in the Appendix, full account was taken of hfs splitting for the Eu II transitions; the La II lines were so weak in HD 122563 that hfs compensation was not needed. Second synthesis attempts were made after use of these line lists in the synthesis of the solar spectrum. For the solar-spectrum matching, we again employed the Liège solar atlas and the Holweger and Müller (1974) solar model. Oscillator strengths of all transitions with lab *gf*-values were held fixed, and the *gf*-values of the other features were altered to obtain the best fit to the solar spectrum. These altered line lists were then again used to synthesize the spectrum of HD 122563. In general the force-fits to the solar spectrum provided little change to the appearance of the synthesized HD 122563 spectrum, for the features of our star are dominated by a few strong lines for which lab *gf*-values have been obtained.

In Figures 4 and 5 we show a few examples of the synthetic spectrum fits for HD 122563, and the final abundances for the rare earths are given in Table 2. It is clear from the figures and table that the *s*-process elements are very overdeficient in the star, and that the *r*-process elements also may be somewhat more deficient than the iron-peak elements. This result did not change significantly upon use of the model derived from the differential analysis (see the discussion of errors below).

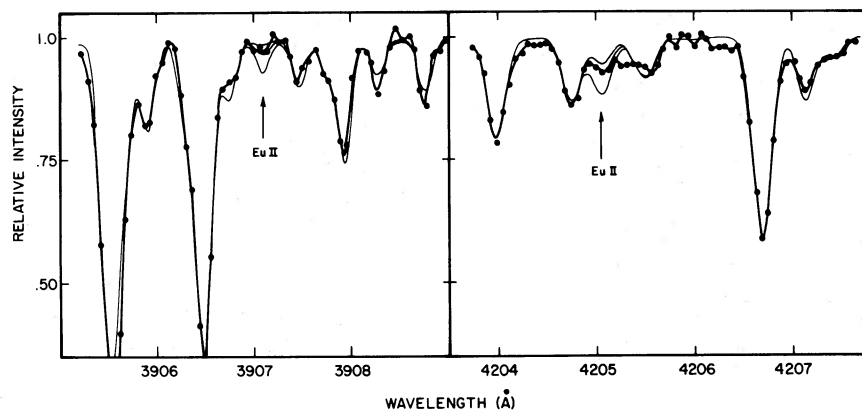


FIG. 4.—Synthetic and observed HD 122563 spectra of two Eu II features. The observations are represented by the thick line connecting the actual data points. The synthetic spectra have been generated with the low-temperature model, iron-peak element abundances derived in this study, and with  $[Eu/Fe] = +0.0, -0.4, \text{ and } -0.8$ .

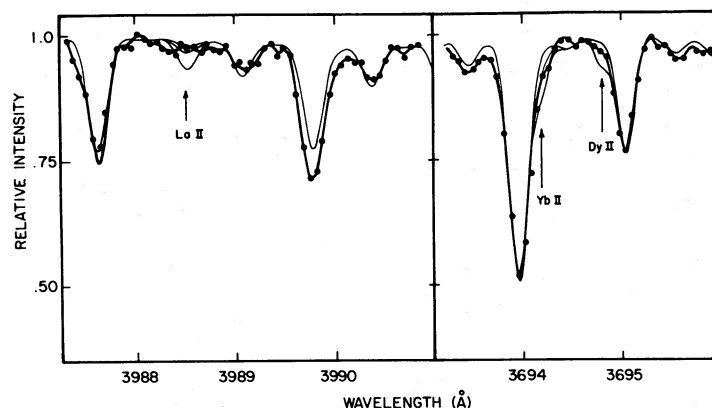


FIG. 5.—Synthetic and observed HD 122563 spectra for other  $s$ - and  $r$ -process lines. Observed spectra are represented as in Fig. 4, and the element ratios with respect to Fe in the synthetic spectra are identical to those listed for Fig. 4.

Error estimates for all abundances may be obtained from the entries in Table 4. To generate this table, we computed metal abundances using a wide variety of standard model atmospheres from the Bell *et al.* (1976) grid. The grid models chosen for these computations represent extreme values of the uncertainties possible for model parameters in HD 122563. The test line parameters were matched to typical parameters for the computed species lines. Most computations were carried out for moderately weak test lines,  $\log(W/\lambda) = -5.2$ ; as noted before, most real absorption features in the spectrum of HD 122563 are unsaturated. We note from Table 4, following the work of many earlier investigators in the field, that the ratios of element abundances derived from lines of similar excitation potentials from the same species of elements with similar ionization potentials (e.g.,  $[Zr/Ti]$ ) are particularly insensitive to model atmosphere uncertainties. These same ratios also should minimize the uncertainties arising from departures

from LTE in the atmosphere of HD 122563. The model parameter dependencies of Table 4 along with the stated atmosphere uncertainties listed in Table 2 clearly show that abundance ratios of interest in HD 122563 suffer no large errors due to atmosphere uncertainties. Exceptions obviously occur for species which have observable features only on the damping portion of the curve of growth. Sr II, for instance, exhibits resonance lines with equivalent widths  $\log(W/\lambda) = -4.43$  and  $-4.41$ . The entries in Table 4 for strong lines demonstrate the great sensitivity of the Sr abundance to the adopted microturbulence; this abundance should be interpreted with caution.

Finally, Table 4 shows the effects of alteration of the source function in the computations. Large departures of the continuum mean intensity  $J$  from the Planck function  $B$  occur in stellar atmospheres at small optical depths, especially at wavelengths far from the flux peaks (e.g., see Hinkle and Lambert 1975). In principle this

TABLE 4  
ABUNDANCE CHANGES FOR TYPICAL LINES OF VARIOUS SPECIES

$T_{\text{eff}}/\log g/[M/H]/v_{\text{turb}}$	Ti I 0.50 <sup>a</sup>	Ti II 1.00 <sup>a</sup>	Fe I 0.00 <sup>a</sup>	Fe I 3.00 <sup>a</sup>	Fe II 2.80 <sup>a</sup>	Y II 0.50 <sup>a</sup>	Eu II 0.00 <sup>a</sup>	<i>r, s/M</i>
4500/0.75/−3.0/2.3	+0.00 <sup>b,c</sup>	+0.00	+0.00	+0.00	+0.00	+0.00	+0.00	+0.00
4500/0.75/−3.0/1.5	+0.09	+0.07	+0.08	+0.09	+0.09	+0.10	+0.10	+0.02
4500/0.75/−3.0/1.5 (log $W/\lambda$ ) = −4.6	+0.69	+0.66	+0.59	+0.51	+0.65	+0.69	+0.75	...
4500/0.75/−3.0/3.5	−0.05	−0.05	−0.05	−0.06	−0.05	−0.05	−0.06	+0.00
4500/0.75/−3.0/3.5 log $W/\lambda$ = −4.6	−0.73	−0.69	−1.00	−0.71	−0.73	−0.77	−0.80	...
4500/0.75/−3.0/2.3 $S(\text{line}) = S(\text{cont}) = J(\text{cont})$	+0.09	+0.07	+0.08	+0.10	+0.10	+0.08	+0.06	−0.02
4500/0.75/−3.0/2.3 $S(\text{line}) = B, S(\text{cont}) = J(\text{cont})$	−0.01	−0.03	−0.03	−0.02	−0.01	−0.03	−0.04	−0.02
4500/0.75/−2.0/2.3	−0.18	+0.00	−0.26	−0.14	−0.01	+0.01	+0.00	+0.01
4500/1.50/−3.0/2.3	−0.21	+0.10	−0.21	−0.20	+0.12	+0.10	+0.10	+0.00
4500/1.50/−2.0/2.3	−0.36	+0.17	−0.40	−0.31	+0.16	+0.18	+0.17	+0.01
4000/1.50/−2.0/2.3	−1.36	+0.15	−1.37	−0.80	+0.48	+0.07	+0.00	−0.28
5000/1.50/−2.0/2.3	+0.37	+0.34	+0.56	+0.16	+0.12	+0.41	+0.46	+0.20
5000/1.50/−3.0/2.3	+0.39	+0.33	+0.56	+0.20	+0.11	+0.40	+0.45	+0.19

<sup>a</sup>Excitation potential.

<sup>b</sup>All abundance changes are relative to those of the 4500/0.75/−3.0/2.3 model.

<sup>c</sup>Unless otherwise noted, abundances were computed for lines of fairly weak strength:  $\log(W/\lambda) = -5.20$ .

could affect the relative abundances from ultraviolet and red transitions in HD 122563. However, the influence of Rayleigh scattering keeps ultraviolet continuous opacities in this star large at small reference Rosseland mean optical depths. Therefore  $J$  and  $B$  are nearly equal through most of the atmosphere at ultraviolet wavelengths; lines are effectively formed near the continuum of this star regardless of wavelength, and, as expected, only minor variations in abundances are seen with different source function assumptions.

## V. DISCUSSION

The derived abundances for HD 122563 are displayed in Figure 6. From the preceding sections a pattern has emerged of greatly depleted *s*-process elements and mildly deficient *r*-process elements with respect to the iron group of elements. Here we shall attempt to indicate probable outlines of the nucleosynthesis history of the heavy elements in stellar generation(s) prior to the formation of HD 122563. In this discussion a few points

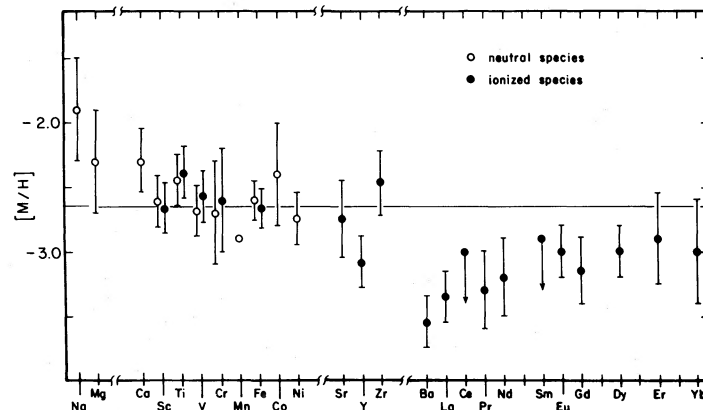


FIG. 6.—Element abundances in HD 122563. The lower temperature model was employed for these abundances.

should be emphasized: (a) the lack of isotopic information for the heavy elements; (b) the large errors assessed for a few of the element abundances; and (c) the inability of our study to determine unambiguously whether or not HD 122563 has undergone its own synthesis of the  $s$ -process elements. As mentioned briefly in § I, the peculiar light-element abundance and isotopic ratios, combined with derived atmosphere parameters and H-R diagram position of this star, strongly suggest an evolved, chemically mixed star. However, the large overdeficiency of the heavier  $s$ -process elements in HD 122563 demands that any of these elements which may have been generated in the interior of this star make little contribution to the overall observed abundance pattern, and thus may be ignored in most of the arguments presented below.

A first task in any heavy-element nucleosynthesis study is the assignment of relative contributions of the  $r$ - and  $s$ -process fractions to each element. For this we consider some simple limiting cases involving exclusive  $s$ -processing, exclusive  $r$ -processing, or a linear combination of them. In Table 5 we have listed abundance data in the Sun and HD 122563 for the relevant atoms, as well as the breakdown of solar system  $r$ - and  $s$ -process contributions to each element (Cameron 1982). The remaining columns of this table contain predicted abundances for HD 122563 assuming various nucleosynthesis

histories. Critical element ratios for the evaluation of nucleosynthesis models are Sr, Y, or Zr to Ba, and Ba to Eu. The first ratio involves three elements near the  $s$ -process peak near magic neutron number  $N = 82$ , and one element near the  $s$ -process peak near  $N = 126$ . The second ratio compares an element near  $N = 126$  which almost exclusively is made via the  $s$ -process in the solar system, to one element made nearly completely by the  $r$ -process.

The entries for models 2 and 3 in Table 5 demonstrate convincingly that the  $s$ -process cannot account for the major features of the heavy-element distribution in HD 122563. Model 2 assumes that the  $s$ -process but not the  $r$ -process was active in the early galactic history, and further assumes that the ratios of the isotopes which formed the solar system  $s$ -process abundances are identical to the ratios in HD 122563. We chose to normalize this distribution to the well-determined Ba abundance, and scaled all other element contents appropriately. As one example, to get the predicted lanthanum abundance for model 2 we first note that  $\log \epsilon_{\odot}(\text{Ba}) = 2.09$  and  $\log \epsilon_{\odot}(\text{La}) = 1.13$ . We have derived an actual stellar abundance of  $\log \epsilon_{\text{HD122563}}(\text{Ba}) = -1.45$ , and, if we assume only  $s$ -process contributions in the solar ratios to the Ba and La contents of this star and normalize to the observed Ba content, then  $\log \epsilon_{\text{HD122563}}(\text{La}) = -1.45 - (2.04 - 0.94) = -2.55$ . The scaled solar-system  $s$ -process

TABLE 5  
 $r$  AND  $s$  CONTRIBUTIONS TO THE ABUNDANCES

ELEMENT	% $r^a$	% $s^a$	$\log \epsilon(\text{H} = 12)$					
			Sun	122563	(1)	(2)	(3)	(4)
Sr.....	8.4	91.6	2.90	+0.15	-1.14	-0.63	-0.01	-0.07
Y.....	27.1	72.9	2.24	-0.84	-1.30	-1.39	-0.61	-0.61
Zr.....	20.9	79.1	2.56	+0.11	-1.08	-1.03	-0.23	-0.26
Ba.....	11.6	88.4	2.09	-1.45	-1.81	-1.45	-1.45	-1.36
La.....	35.1	64.9	1.13	-2.22	-2.28	-2.55	-2.60	-2.14
Ce.....	19.4	80.6	1.55	< -1.5	-2.12	-2.03	-2.35	-1.95
Pr.....	52.8	47.2	0.99	-2.3::	-2.25	-2.83	-3.44	-2.23
Nd.....	31.8	68.2	1.26	-1.9::	-2.20	-2.40	-2.93	-2.14
Sm.....	62.8	37.2	0.80	< -2.4	-2.36	-3.12	-3.69	-2.34
Eu.....	91.5	8.5	0.51	-2.49	-2.49	-4.05	-4.90	-2.49
Gd.....	79.2	20.8	1.12	-2.03:	-1.94	-3.04	-3.98	-1.94
Dy.....	76.1	23.9	1.06	-1.94	-2.02	-3.05	-3.84	-2.01
Er.....	72.8	27.2	0.76	-2.1::	-2.34	-3.10	-4.05	-2.33
Yb.....	56.1	43.9	0.9	-2.1::	-2.31	-2.20	-3.91	-2.30

<sup>a</sup>Solar system.

Model 1.—A scaled distribution of only the  $r$ -process contributions to the solar system abundances of the elements. The distribution is normalized to the derived Eu abundance in HD 122563.

Model 2.—A scaled distribution of only the  $s$ -process contributions to the solar system abundances of the elements. The distribution is normalized to the derived Ba abundance in HD 122563.

Model 3.—Theoretical  $s$ -process distribution normalized to Ba in HD 122563. A single neutron exposure with  $\tau = 0.80$  is adopted (Cowley and Downs 1980).

Model 4.—The  $r$ -process abundances of model 1 combined with the  $s$ -process abundances, lowered by 0.1 dex, of model 3.

distribution derived in this manner fails in almost every respect for our star, particularly in its underproduction of the Sr-Y-Zr elements and of the Eu and heavier elements. More generally we can find no *s*-process synthesis which matches the observed heavy element contents in HD 122563. For example, model 3 in Table 5 shows the element ratios of a theoretical model (Cowley and Downs 1980) specifically chosen to match the Sr-Y-Zr/Ba ratios of our star. This single neutron exposure model of necessity is one with a short total neutron exposure  $\tau$ ; longer exposures tend to increase the relative abundances of the heavy *s*-process elements at the expense of the lighter ones. This theoretical model does not account for the abundances of any element near Eu. Additionally an inspection of Table 1 of Cowley and Downs (1980) indicates that no *s*-process model (single exposure or exponential exposure distribution) can reproduce our observed Ba/Eu ratio. Those authors point out that at low exposures the relative enhancement seen in Eu is very small, while at high exposures Eu is manufactured but quickly destroyed due to the high neutron capture cross sections of both of its major isotopes; thus the Ba/Eu ratio will stay at large values irrespective of the details of the particular *s*-process model. The *s*-process therefore is rejected for the major heavy element synthesis in HD 122563.

A more promising model is one which presumes *r*-process nucleosynthesis only. This possibility has been suggested recently by Truran (1981*a*). The details of the *r*-process, as pointed out by many workers in the field, are known more poorly than those of the *s*-process. However, model 1 of Table 5, which assumes a pure *r*-process with isotope ratios identical to those of the solar system, produces much closer fits to the heavy-element abundances of our star. For model 1 we chose to normalize abundances to the stellar Eu value, yet many elements on either side of Eu are matched well. Some additional features of this model appear to complicate the picture. First, in order to match the Eu abundance we of course were forced to assume an overdeficiency of the *r*-process elements, as derived previously in the paper. Note, however, that this scale factor also serves to reproduce well the abundance of the classic *s*-process elements such as La and Pr. Second, the model does not appear to produce either the light *s*-process elements Sr, Y, and Zr or the heavy element Ba; since Zr and Ba exhibit solar system abundances completely dominated by the *s*-process, these results are hardly surprising. Moreover, Truran (1981*a*) has pointed out that the larger than solar Y/Ba ratios characteristic of HD 122563 and other extremely metal-deficient stars actually can argue in favor of a pure *r*-process origin for these elements. One persistent feature of *r*-process calculations is the great sensitivity to initial seed nuclei contents, of the resulting abundance ratios of elements near  $N = 82$  to those near  $N = 126$ . Specifically, to re-

produce the *r*-process fractions of the solar system abundances of Ba and Zr it is necessary to postulate not pure Fe seeds before an *r*-process episode, but rather a significant amount of *s*-processing to heavier elements first (Cowan, Cameron, and Truran 1980; Truran 1981*b*). A pure *r*-process event with Fe-peak seeds underproduces the elements near Ba. This fits quite well with our requirements: we see little evidence for the *s*-process in the heavier elements, and require a large Y/Ba ratio. Figure 2 of Cowan, Cameron, and Truran (1980) demonstrates that the needed light/heavy ratios can be produced quite easily from variation of the assumed amount of *s*-processing prior to onset of the *r*-process. Finally, the observed deficiency of the Eu/Fe ratio is not a problem with this model; only if this ratio were anomalously *large* would the pure *r*-process scenario have trouble.

The underproduction of Ba relative to Eu in the *r*-process is somewhat troubling, so we consider one additional possibility: almost all heavier elements may be manufactured via the *r*-process, while the *s*-process creates the elements Sr, Y, Zr, and to some extent Ba. Truran and Iben (1977) have suggested that the large ratios of Sr/Ba seen in earlier metal-poor star data may be understood in terms of massive star evolution. Presumably the stellar generation(s) which produced material for HD 122563 were massive stars, for our star surely was born near the beginning of the Galaxy. Massive progenitor stars can produce some *s*-process products during core helium burning using neutrons produced from  $^{22}\text{Ne}$ , but only the lighter *s*-process elements are made in large quantities. This is because of the presence of significant numbers of neutron poisons in the  $^{22}\text{Ne}$  burning regions (Couch, Schmiedekamp, and Arnett 1974; Lamb *et al.* 1977). Also, if the site of this *s*-process is core He-burning, the number of total available neutrons is limited by the original amount of  $^{14}\text{N}$  which is converted to  $^{22}\text{Ne}$ ; fresh  $^{14}\text{N}$  fuel will not be constantly added from He-burning layers as in the case of repeated shell flash synthesis. Therefore the nucleosynthesis which preceded the formation of HD 122563 may have been a short *s*-process event in the core helium burning of a massive star ( $M > 30 M_{\odot}$ ) followed by the explosive *r*-process episode during the stellar supernova. A simple model of the resulting element mix is given in model 4 of Table 5. To produce model 4 we have added the pure *r*-process model 1 together with the theoretical *s*-process model 3 which has been scaled down by 0.1 dex uniformly for all elements. Nearly all elements from Sr through Yb are matched to within observational errors with this *r*- and *s*-process combination. It is tempting to speculate that the small amount of *s*-processing used in this model also provides the necessary seeds for the subsequent explosive *r*-process. More detailed models are unwarranted here, but a consistent solution for nucleosynthesis

emerges from the abundances in HD 122563: two separate but related neutron capture episodes in the very massive metal-poor progenitors of Population II stars.

The preceding discussion has assumed an essentially primary origin for the  $r$ -process elements in HD 122563. It is worth noting that it is possible to explain the lower than solar Eu/Fe ratio by assuming that the solar system  $r$ -process elements were produced partly in secondary nucleosynthesis events. Cowan, Cameron, and Truran (1982) have pointed out that helium shell flashes in low-mass stars can, under certain conditions, reproduce the solar system  $r$ -process distribution. A low-mass component to the  $r$ -process synthesis in the Galaxy would naturally lead to an underabundance of the  $r$ -process elements in the early generations of the Galaxy. Of course, since a variety of Y/Eu and, hence, Fe/Eu ratios are possible from standard explosive  $r$ -process computations (Cowan, Cameron, and Truran 1980), no quantitative estimate can be put on the secondary low-mass  $r$ -process importance at the present time.

Important observational work remains for the heavy elements in metal-poor stars. First, the question of the apparent scatter in Eu from star to star must be cleared up. If the scatter is real, the relationship between Eu, Ba, and the Y group of elements ought to help define the limits of the nucleosynthesis which occurred before the Population II stars were formed, and indeed may define the time between the first onset of galactic star formation and the birth of today's Population II stars. Second, cool Population II dwarfs should be studied more exten-

sively. This paper has suggested that the progenitors of HD 122563 underwent some short-lived mild  $s$ -processing which enhanced their Sr-Y-Zr group of elements. However, we are unable to prove that these elements have not been manufactured by our star itself. Detailed studies of dwarf stars cool enough to show appreciable features of the rare earths should clarify this problem. Finally, special studies should be undertaken on stars such as the intriguing HD 115444. Griffin *et al.* (1982) have shown this cool Population II giant to have greatly enhanced  $s$ -process elements and have labeled this star the first true Population II barium star. However, they were able to study only Ba, La, and Eu among the heavy elements. The present study has shown that data for more elements can lead to understandable nucleosynthesis histories for the very metal-poor HD 122563, and we suspect that HD 115444 holds similar clues in its rare earth elements.

We are grateful to J. Brown for assistance in gathering the observational material for this study. S. Parsons and J. Dominy provided valuable advice and computer routines to help with the data analysis. We thank D. L. Lambert, J. Tomkin, J. W. Truran, F. N. Bash, J. N. Scalo, and J. C. Wheeler and referee R. E. Luck for useful conversations and helpful comments on the manuscript. This work has been supported by NSF grant AST-8100241 to C. S. Financial support from McDonald Observatory to M. P. is gratefully acknowledged.

## APPENDIX

In this section we give the basic line data for HD 122563 and briefly discuss the choices of oscillator strengths (see Table 6). Laboratory measurements have been obtained from literature sources which date usually from the mid-1960s onward. Experimental oscillator strengths determined prior to those years often are unreliable; the classic case, of course, was the necessity to revise Fe I  $gf$ -values by about a factor of 10 from the Corliss and Bozmann (1962) and the Corliss and Tech (1968) results. In spite of the great advances in the accuracy of these lab  $gf$ -values, some species are still in need of work. A critical evaluation of oscillator strengths is beyond the scope of this paper; the following comments should help the reader's understanding of our particular decisions for the various atomic species.

Na I, Mg I. These elements are not of primary interest for the present paper, and we merely adopt the  $gf$ 's recommended in the new critical compilation from the NBS (Wiese and Martin 1980). Although four lines of Mg I were measured in HD 122563, we are prevented from computing a reliable abundance by the lack of  $gf$ 's for two of the lines.

Ca I. For most transitions we employed the new very accurate laboratory transition probabilities of Smith and Raggett (1981). Use of these  $gf$ -values leads to a consistent solar Ca abundance for all lines (Smith 1981). For the few Ca I lines in our sample not studied by Smith and Raggett (1981), we used the values of Holweger (1972). That set of oscillator strengths has generally lower accuracy (Holweger 1972; Lambert and Luck 1978), and we assigned lower weight to those transitions.

Ti I, Ti II. Many laboratory investigations of the oscillator strengths for neutral titanium have been conducted; the agreement of the  $gf$ -values for lines in common among the samples is very good. Only one extensive set of experimental results exists for Ti II (Roberts, Anderson, and Sorenson 1973*a*), and this set is adopted.

V I, V II. The oscillator strength scale for vanadium is not well established. The compilation of Wiese and Martin (1980), from which we have taken the V I  $gf$ 's, lists their uncertainties as within 50%. A large number of experimental  $gf$ -values for V II have been published by

TABLE 6  
LINE DATA FOR HD 122563

Wavelength	Species	RMT	E. P.	Log(gf)	Source	E.W. <sup>0</sup> sun	E.W. <sup>c</sup> star	Wavelength	Species	RMT	E. P.	Log(gf)	Source	E.W. sun	E.W. star
6160.75	Na I	5	2.10	-1.23	1	53.5	6	4913.62	Ti I	157	1.87	-.03	8	45.0	4
4167.27	Mg I	15	4.34				57	4981.74	Ti I	38	0.85	.40	12	104.1	62
4571.02	Mg I	1	0.00			99.2	85	4991.07	Ti I	38	0.85	.32	9,12	100.8	72
5172.70	Mg I	2	2.71	-.38	1		183	4999.51	Ti I	38	0.83	.23	9,12	96.0	46
5183.62	Mg I	2	2.72	-.16	1		217	5147.48	Ti I	4	0.00	-1.97	6,8	34.6	8
4108.52	Ca I	39	2.71			65.2	8	5173.75	Ti I	4	0.00	-1.14	6,8,10		29
4425.44	Ca I	4	1.88	-.36	1		52	5192.98	Ti I	4	0.02	-1.04	6,8,10	76.3	38
4578.84	Ca I	23	2.52	-.70	36	77.6	9	5210.39	Ti I	4	0.05	-1.04	6,8,10	78.2	46
5261.70	Ca I	22	2.52	-.58	36	98.2	18	5866.46	Ti I	72	1.07	-.92	9,10	43.6	7
5857.46	Ca I	47	2.93	-.24	36	125.3	26	3456.39	Ti II	99	2.06	-.79	3		75
6122.23	Ca I	3	1.89	-.43	2,2	173.9	62	3480.89	Ti II	22	1.08	-.16			59
6161.30	Ca I	20	2.52	-1.27	36	60.5	8	3533.87	Ti II	98	2.06	-1.67	3		59
6162.18	Ca I	3	1.90	-.25	2	213.3	78	3648.79	Ti II	74	1.57				12
6439.08	Ca I	18	2.52	+3.9	36	148.5	55	3641.33	Ti II	52	1.24	-.71	3		101
6449.82	Ca I	19	2.52	-.50	36	96.2	16	3659.76	Ti II	75	1.58	-.86	3	95.9	78
6455.61	Ca I	19	2.52	-1.29	36	53.7	8	3759.30	Ti II	13	0.61	-.22	3		183
6471.67	Ca I	18	2.52	-.69	36	87.7	23	3776.06	Ti II	72	1.58	-1.24	3	92.0	60
6493.78	Ca I	18	2.52	-.11	36	115.5	51	3987.61	Ti II	11	0.61	-2.64	3	49.9	49
6499.65	Ca I	18	2.52	-.82	36	82.9	16	4012.39	Ti II	11	0.57	-1.63	3		108
4020.40	Sc I	7	0.00	-.20	1	43.8	9	4028.35	Ti II	87	1.89	-1.18	3,8	87.0	62
4023.69	Sc I	7	0.02	.32	1	49.0	6	4056.20	Ti II	11	0.61			30.7	23
3535.73	Sc II	11	0.31	-.33	1		92	4163.65	Ti II	105	2.59	-.40	3	105.9	47
3567.70	Sc II	3	0.00				116	4184.31	Ti II	21	1.08			73.2	35
3645.31	Sc II	2	0.02				133	4316.80	Ti II	94	2.05			44.4	18
3651.80	Sc II	2	0.01				136	4330.25	Ti II	94	2.05			40.9	19
3666.54	Sc II	2	0.02			74.8	59	4330.71	Ti II	41	1.18			63.3	51
3923.50	Sc II	9	0.31	.31	1		11	4337.93	Ti II	20	1.08	-2.35	3		103
4246.84	Sc II	7	0.31			146.7	130	4394.07	Ti II	19	1.08	-1.07	3	74.4	71
4354.62	Sc II	14	0.61			57.6	47	4395.85	Ti II	61	1.24	-2.21	3	64.7	55
4415.56	Sc II	14	0.60				76	4409.53	Ti II	61	1.23			37.7	21
4670.41	Sc II	24	1.36	-.39	1	61.3	40	4417.72	Ti II	40	1.16	-1.37	3	96.1	95
5239.82	Sc II	26	1.45	-.76	1	47.7	30	4421.94	Ti II	93	2.06			128.7	118
5657.88	Sc II	29	1.51	-.51	1	66.5	35	4443.81	Ti II	19	1.08	-.81	3	44.0	17
5669.04	Sc II	29	1.50			31.7	8	4444.56	Ti II	31	1.12	-2.37	3	57.8	48
3717.40	Ti I	17	0.00	-1.17	6,7	51.2	21	4468.50	Ti II	31	1.13	-.77	3	127.9	126
3904.79	Ti I	56	0.90				30	4545.14	Ti II	30	1.13			44.2	37
3924.53	Ti I	13	0.02	-.98	6,7,8,9,10		35	4563.77	Ti II	50	1.22	-.90	3	113.5	113
3998.64	Ti I	12	0.05	-.10	6,7,9,10,11	116.8	71	4568.33	Ti II	60	1.22	-2.70	3	26.5	16
4185.13	Ti I	129	1.50	-.14	7	40.9	9	4571.98	Ti II	82	1.57			131.1	111
4321.66	Ti I	235	2.24			34.7	7	4636.32	Ti II	38	1.16			51.8	8
4533.25	Ti I	42	0.85			51.8	54	4657.20	Ti II	59	1.24			48.2	38
4534.79	Ti I	42	0.84			86.9	45	4865.62	Ti II	29	1.12	-2.74	8	35.5	27
4548.77	Ti I	42	0.83	-.29	7	71.5	23	5129.16	Ti II	86	1.89	-1.51	3	73.7	47
4656.47	Ti I	6	0.00	-1.27	10	69.4	27	5154.08	Ti II	70	1.57	-1.92	3	67.4	40
4840.88	Ti I	53	0.90	-.59	8	65.2	25	5185.91	Ti II	86	1.89	-1.51	8	60.7	44

TABLE 6—Continued

Wavelength	Species	RMT	E.P.	Log(gf)	Source	E.W. sun	E.W. star	Wavelength	Species	RMT	E.P.	Log(gf)	Source	E.W. sun	E.W. star
5336.79	Ti II	69	1.58			54.7	47	3451.92	Fe I	81	2.22				82
5381.03	Ti II	69	1.57			66.8	37	3462.36	Fe I	79	2.20				21
6491.58	Ti II	91	2.06			42.1	16	3522.27	Fe I	326	2.83	-1.11	16		42
3844.48	V I	7	0.00				13	3530.39	Fe I	326	2.81	-1.04	16		43
4104.75	V I	112	1.95	.58	1		6	3536.57	Fe I	329	2.87	.05	15		78
4105.16	V I	27	0.27		1		9	3540.13	Fe I	329	2.86	-0.91	15,16		45
4111.79	V I	27	0.30	.36	1	98.6	29	3541.10	Fe I	326	2.85	.15	15		86
4115.17	V I	27	0.29	.08	1	86.4	15	3543.68	Fe I	734	3.41	-0.75	16		24
4123.51	V I	27	0.27	-.32	1	71.0	6	3544.63	Fe I	239	2.61	-1.81	16		24
4128.10	V I	27	0.28	-.15	1	101.1	25	3546.21	Fe I	183	2.43				12
4332.83	V I	5	0.02				7	3549.87	Fe I	48	1.61	-2.51	16		48
4406.65	V I	22	0.30	-.26	1	80.5	12	3630.36	Fe I	323	2.85	-.91	16		40
3517.31	V II	6	1.13	-.33	4		79	3632.56	Fe I	437	2.95	-.96	16		32
3530.78	V II	5	1.07	-.56	4		68	3651.47	Fe I	295	2.76	.09	15		84
3538.26	V II	4	1.13	-1.56	4		27	3658.55	Fe I	231	2.56	-2.47	16		13
3545.19	V II	5	1.10	-.37	4		75	3659.52	Fe I	180	2.45	-.91	15		72
3884.84	V II	33	1.79	-1.44	4		11	3667.26	Fe I	570	3.21	-.69	16		41
3896.14	V II	10	1.40	-1.54	4		25	3684.12	Fe I	292	2.73	-.12	15		64
3916.41	V II	10	1.43	-1.15	4		36	3701.10	Fe I	385	3.00	-.06	15,17,18		74
4002.93	V II	9	1.43	-1.46	4	81.0	36	3707.05	Fe I	385+	3.00				59
4005.71	V II	32	1.82	-.47	4	87.3	17	3715.92	Fe I	124	2.28	-1.43	15,16		56
4023.38	V II	32	1.80	-.62	4	63.0	37	3728.67	Fe I	227	2.56	-1.62	16		21
4036.77	V II	9	1.48	-1.57	4	33.2	15	3731.38	Fe I	225	2.61	-1.30	15,16		35
4183.46	V II	37	2.05	-1.07	4		15	3756.07	Fe I	74	2.18	-2.05	16		27
3639.84	Cr I	47	2.54	.41	5		17	3756.94	Fe I	805	3.57	-.23	15,16		31
4545.96	Cr I	10	0.94	-1.38	5,13,14	78.5	16	3760.54	Fe I	76	2.22	-1.23	15,16		8
4580.06	Cr I	10	0.94	-1.62	5,13,14	76.7	19	3766.09	Fe I	226	2.59	-2.10	16		15
4646.17	Cr I	21	1.03	-.79	13,14	99.0	37	3773.70	Fe I	386	3.04	-1.39	16		9
4651.29	Cr I	21	0.98	-1.52	13	76.3	18	3777.07	Fe I	432	2.99	-1.64	15,16		11
4652.17	Cr I	21	1.00	-1.23	13	96.6	27	3781.19	Fe I	74	2.20	-1.87	16		40
4942.48	Cr I	9	0.94	-2.38	13	180.4	9	3782.45	Fe I	388	3.00	-1.68	16		17
5206.04	Cr I	7	0.94	.03	1	86.9	17	3781.94	Fe I	917	3.64	-1.19	16		9
5298.28	Cr I	18	0.98	-1.39	4	105.0	23	3786.68	Fe I	22	1.01	-2.13	15,16		103
5329.15	Cr I	94	2.91	-.04	4	62.9	9	3791.51	Fe I	223	2.56	-2.06	16		15
5345.81	Cr I	18	1.00	-1.07	13,14	107.2	29	3791.75	Fe I	703	3.42	-1.33	16		10
5348.33	Cr I	18	1.00	-1.36	13,14	90.5	15	3792.83	Fe I	74	2.22	-2.40	16		17
4054.11	Cr II	19	3.10	-2.61	4	47.8	5	3802.29	Fe I	666	3.30	-1.21	16		11
4111.00	Cr II	18+26	3.10	-2.21	4	43.3	5	3804.02	Fe I	702	3.33	-.97	15,16		19
4588.65	Cr II	44	4.07	-.69	13	74.3	22	3805.35	Fe I	608	3.30	.42	15,19		53
4848.25	Cr II	30	3.86	-1.40	4	56.8	13	3821.19	Fe I	608	3.27	.28	15,18		78
5237.32	Cr II	43	4.07	-1.32	4	50.2	7	3852.58	Fe I	73	2.18	-1.17	15		76
4082.94	Mn I	5	2.18	-.26	1		10	3891.93	Fe I	733	3.41	-.55	15,16		21
4823.51	Mn I	16	2.32	.10	1	132.1	35	3907.94	Fe I	280	2.76	-1.04	15,16		50
3450.33	Fe I	82	2.22	-.89	15		91	3916.74	Fe I	606	3.24	-.50	15,16		35

TABLE 6—Continued

Wavelength	Species	RMT	E.P.	Log(gf)	Source	E.W. sun	E.W. star	Wavelength	Species	RMT	E.P.	Log(gf)	Source	E.W. sun	E.W. star
3995.99	Fe I	279	2.73	-1.40	15,16	80.0	33	4222.22	Fe I	152	2.45	-0.93	15	150.4	77
4001.67	Fe I	72	2.18	-1.84	15,16	86.6	41	4225.46	Fe I	693	3.42	-0.47	15		45
4011.72	Fe I	153	2.45	-2.67	16	43.9	6	4225.96	Fe I	521	3.05	-1.33	15		25
4062.45	Fe I	359	2.84	-0.76	15	101.6	45	4227.44	Fe I	693	3.33	.27	15		95
4063.61	Fe I	43	1.56	.11	15,19		174	4232.73	Fe I		0.11			48.7	36
4067.28	Fe I	217	2.56	-1.37	15	89.9	44	4233.61	Fe I	152	2.48	-0.55	15	207.8	89
4070.78	Fe I	558	3.24	-0.76	15,16		37	4238.03	Fe I	689+	3.42			104.3	28
4071.75	Fe I	43	1.61	-.02	15,19,20		167	4238.82	Fe I	693	3.40			149.5	42
4073.77	Fe I	558	3.26	-.84	15,16	82.7	28	4337.06	Fe I	41	1.56	-1.25	15		103
4079.84	Fe I	359	2.86	-1.27	15,16	80.9	24	4347.24	Fe I	2	0.00	-5.70	15,20	34.4	20
4080.22	Fe I	558	3.28	-1.16	15,16	78.4	20	4348.95	Fe I	414	2.99	-2.09	16	51.4	7
4084.50	Fe I	698	3.33	-.57	15	133.9	51	4387.90	Fe I	476	3.07	-1.43	16	72.8	13
4089.22	Fe I	422	2.95	-1.91	15,16	55.2	11	4388.41	Fe I	830	3.60	-0.58	15	99.4	27
4091.56	Fe I	357	2.83	-2.08	15,16	52.1	8	4389.25	Fe I	2	0.05	-4.58	16,22	66.8	56
4104.94	Fe I	694	3.33	-.41	15,16	66.3	15	4415.14	Fe I	41	1.61	-.62	15,20		135
4109.06	Fe I	558	3.29	-1.16	15,16	85.5	34	4445.48	Fe I	2	0.09	-5.44	16,22	35.1	12
4114.45	Fe I	357	2.83	-1.16	15,16	85.5	34	4461.66	Fe I	2	0.09	-3.21	22	122.3	119
4114.94	Fe I	695	3.37	-1.59	16	59.1	9	4484.23	Fe I	828	3.60			91.9	20
4120.21	Fe I	423	2.99	-1.13	15,16,18	84.1	29	4489.75	Fe I	2	0.12	-3.97	16,22	86.1	85
4126.19	Fe I	595	3.33	-.89	16	98.8	22	4574.73	Fe I	115	2.28	-2.94	16,17	54.1	10
4134.69	Fe I	357	2.83	-.46	15	125.4	60	4630.13	Fe I	115	2.28	-2.54	16,17	69.2	15
4136.53	Fe I	694	3.37	-1.47	16	72.7	11	4635.85	Fe I	349	2.84	-2.39	16	51.9	5
4137.00	Fe I	726	3.41	-.52	15	83.7	31	4637.51	Fe I	554	3.28	-1.33	16	82.4	12
4137.42	Fe I	1103	4.28	-.89	16	54.2	9	4643.47	Fe I	820	3.65	-1.23	16	68.4	7
4139.94	Fe I	18	0.99	-3.63	16,21	77.3	40	4647.44	Fe I	409	2.95			82.2	25
4146.07	Fe I	422	2.99	-1.81	15,16		10	4678.85	Fe I	821	3.60			97.5	19
4147.68	Fe I	42	1.48	-2.10	15,20	103.4	80	4871.33	Fe I	318	2.86	-.38	15	202.0	86
4150.25	Fe I	695	3.43	-1.19	16	70.7	15	4872.14	Fe I	318	2.88	-0.58	15	159.5	67
4154.81	Fe I	694	3.37	-.34	15	128.2	47	4890.76	Fe I	318	2.87	-0.40	15	233.3	86
4157.79	Fe I	695	3.42	-.65	16	120.2	42	4891.50	Fe I	318	2.85	-1.10	15	275.1	93
4158.80	Fe I	695	3.43	-.65	16	98.0	23	4907.74	Fe I	687	3.43			58.7	11
4174.92	Fe I	19	0.91	-2.97	21		84	4919.00	Fe I	318	2.86	-.34	15	214.0	87
4176.58	Fe I	689	3.37	-.61	15	126.1	36	4924.77	Fe I	114	2.28	-2.17	17	85.6	36
4177.08	Fe I	690	3.33	-1.12	16	24.3	2	4930.31	Fe I	985	3.96	-1.29	16	73.2	10
4182.39	Fe I	476A	3.02	-.50	15	85.8	29	4938.82	Fe I	318	2.87	-3.34	21	117.3	54
4187.05	Fe I	152	2.45	-.50	15	230.2	97	4939.69	Fe I	16	0.86			94.0	79
4187.81	Fe I	152	2.42	-.50	15		103	4946.40	Fe I	687	3.37			95.8	26
4189.57	Fe I	940	3.69	-1.27	16	67.9	8	4966.10	Fe I	687	3.33	-.81	15	114.9	38
4196.21	Fe I	693	3.40	-.71	15,16	103.1	26	4983.26	Fe I	1067	4.15			95.7	12
4199.11	Fe I	522	3.05	-.19	18	180.9	83	4994.14	Fe I	16	0.91	-3.08	21	96.3	92
4202.04	Fe I	42	1.48	-.71	19,20	358.5	138	5123.73	Fe I	16	0.11	-3.07	15,21	102.6	70
4202.76	Fe I	476+	3.02				5	5125.13	Fe I	1090	4.22				23
4207.13	Fe I	352	2.83	-1.40	15,16	77.6	27	5131.48	Fe I	66	2.22			73.7	26
4208.61	Fe I	689+	3.40			87.2	22	5133.70	Fe I	1092	4.18			146.8	31
4220.35	Fe I	482	3.07	-1.24	15,16	78.9	20	5141.75	Fe I	114	2.42			81.0	18

TABLE 6—Continued

Wavelength	Species	RMT	E.P.	Log(gf)	Source	E.W. sun	E.W. star	Wavelength	Species	RMT	E.P.	Log(gf)	Source	E.W. sun	E.W. star
5151.92	Fe I	16	1.01	-3.32	21	94.6	57	6408.03	Fe I	816	3.69			90.4	12
5162.28	Fe I	1089	4.18			140.2	24	6411.66	Fe I	816	3.65			122.6	21
5165.42	Fe I	1089	4.22			76.9	8	6430.86	Fe I	62	2.18			106.5	52
5166.28	Fe I	1	0.00	-4.20	22,23		82	6494.99	Fe I	168	2.40			142.3	77
5171.61	Fe I	36	1.48	-1.79	15,20		95	4002.07	Fe II	29	2.78	-3.65	24	32.5	5
5191.42	Fe I	383	3.04			146.1	53	4087.28	Fe II	28	2.58	-4.93	24	13.2	3
5192.35	Fe I	383	3.00			170.6	63	4128.74	Fe II	27	2.58	-3.55	24	45.1	13
5194.95	Fe I	36	1.56	-2.09	20	118.1	80	4178.86	Fe II	28	2.58	-2.90	24	80.2	58
5195.48	Fe I	1092	4.22			94.2	11	4416.83	Fe II	27	2.78	-2.60	24	80.9	46
5196.07	Fe I	1091	4.26			67.7	10	4541.52	Fe II	38	2.85	-2.93	24	59.3	26
5198.72	Fe I	66	2.22	-2.13	15	90.1	29	4576.34	Fe II	38	2.84	-2.89	24	64.5	26
5215.19	Fe I	553	3.26			115.7	31	4582.83	Fe II	37	2.84	-3.17	24	50.0	19
5216.28	Fe I	36	1.61	-2.15	20	109.5	75	4583.84	Fe II	38	2.81	-1.90	24	109.7	82
5217.40	Fe I	553	3.21			106.7	25	4648.95	Fe II	25	2.58	-4.67	24		4
5225.53	Fe I	1	0.11	-4.79	22,23	69.9	46	4656.75	Fe II	37	2.83	-3.29	24	51.7	19
5232.95	Fe I	383	2.94			269.2	86	4993.35	Fe II	36	2.81	-3.71	24	36.8	16
5242.50	Fe I	843	3.63	-1.3	15,16,17,18	83.6	14	5197.58	Fe II	49	3.23	-2.40	24	76.9	35
5247.06	Fe I	1	0.09	-0.84	15,18		36	5234.63	Fe II	49	3.22	-2.31	24	79.7	40
5250.22	Fe I	1	0.12	-4.94	22,23	62.1	36	5264.81	Fe II	48	3.33	-3.49	24	43.5	9
5250.65	Fe I	56	2.20			63.4	39	5276.00	Fe II	49	3.20	-2.23	24		45
5263.31	Fe I	553	3.26			94.1	38	5264.00	Fe II	41	2.89	-3.50	24	59.8	20
5269.55	Fe I	15	0.86	-1.32	15,21	115.7	21	5284.11	Fe II	74	3.89	-2.89	24	34.2	4
5281.80	Fe I	383	3.04	-0.95	15	135.6	40	6149.25	Fe II	74	3.89	-2.91	24	39.4	8
5307.37	Fe I	36	1.61	-2.99	20	79.1	42	6456.39	Fe II	74	3.90	-2.25	24	62.6	18
5324.19	Fe I	553	3.21			245.6	62	6515.05	Fe II	40	2.89	-3.63	24	56.5	30
5328.05	Fe I	15	0.91	-1.47	15,21		147	3518.35	Co I	36	1.05	.07	25		83
5332.91	Fe I	37	1.56			82.7	105	3529.04	Co I	5	0.17	-.88	25		96
5339.94	Fe I	553	3.26			132.7	40	3564.96	Co I	19	0.58	-.97	25	68.1	106
5364.88	Fe I	1146	4.44	-.67	15	119.4	17	3652.55	Co I	4	0.17	-1.86	25	43.3	7
5365.41	Fe I	786	3.57			73.6	9	3755.45	Co I	96	2.08				
5367.48	Fe I	1146	4.41			128.6	24	3842.05	Co I	33	0.92	-.77	25		63
5383.38	Fe I	1146	4.31	.37	15	162.6	39	4020.91	Co I	16	0.43	-2.07	25	72.2	44
5393.18	Fe I	553	3.24	.52	15,16	131.7	46	4110.54	Co I	29	1.05	-1.08	25	94.9	40
5397.14	Fe I	15	0.91	-.84	15	186.8	129	4121.33	Co I	28	0.92	-.32	25	125.1	91
5859.60	Fe I	1181	4.55	-1.99	15,21	68.7	6	4190.71	Co I	1	0.00		25	54.4	28
5862.37	Fe I	1180	4.55			84.0	10	3551.33	Ni I	5	0.17	-2.28	26		86
6136.62	Fe I	169	2.45			125.8	60	3661.98	Ni I	16	0.21			66.2	63
6137.70	Fe I	207	2.59			119.9	59	3670.43	Ni I	4	0.17	-2.20	26,27		94
6297.80	Fe I	62	2.22			114.9	15	3762.61	Ni I	15	0.21				9
6301.51	Fe I	816	3.65	-2.86	16	66.7	17	3772.53	Ni I	15	0.03			61.3	43
6335.34	Fe I	62	2.20			90.4	33	3778.07	Ni I	15	0.03				51
6336.83	Fe I	816	3.69			104.8	10	3831.70	Ni I	31	0.42	-2.06	26,27		102
6355.04	Fe I	342	2.84			61.2	8	3858.30	Ni I	32	0.42	-.96	26,27		129
6393.61	Fe I	168	2.43	-2.41	16	120.4	57	3912.98	Ni I	15	0.03			46.5	24
								4331.65	Ni I	52	1.68			62.4	9

TABLE 6—Continued

Wavelength	Species	RMT	E.P.	Log(gf)	Source	E.W. sun	E.W. star
4648.66	Ni I	98	3.42	.17	28	79.4	18
4831.18	Ni I	111	3.61	-.07	28	78.2	11
4904.42	Ni I	129	3.54	.13	28	84.3	18
4937.35	Ni I	114	3.61	.21	28	83.7	12
5115.40	Ni I	177	3.83	.21	28	75.4	11
5146.49	Ni I	162	3.70	.12	28	79.0	14
5892.88	Ni I	68	1.99	.15	28	71.0	13
6108.13	Ni I	45	1.68	.15	1	60.8	9
4077.73	Sr II	1	0.00	.15	1		160
4215.54	Sr II	1	0.00	-.17	1		158
3549.02	Y II	9	0.13	-.28	29		57
3774.33	Y II	7	0.13	.21	29		74
3788.70	Y II	7	0.10	-.07	29		73
4358.72	Y II	5	0.10	-1.43	29		35
4398.02	Y II	5	0.13	-1.00	29		34
4883.69	Y II	22	1.08	.07	29	46.2	26
4900.12	Y II	22	1.03	-.09	29	56.9	24
5123.22	Y II	21	0.99	-.83	29	54.1	24
5200.42	Y II	20	0.99	-.57	29	24.2	9
3438.23	Zr II	1	0.09	.11	29	32.1	114
3481.16	Zr II	46	0.80	.11	29		59
3549.53	Zr II	84	1.24	-.40	30		15
3551.94	Zr II	1	0.09	-.31	30		72
3630.03	Zr II	10	0.36	-1.11	30		27
3633.49	Zr II	102	1.75				9
3674.79	Zr II	9	0.32				57
3714.79	Zr II	18	0.53	-.93	30	26.4	23
4161.20	Zr II	42	0.71	-.72	30	55.4	29
4208.99	Zr II	41	0.71	-.46	30	38.0	29
4554.03	Ba II	1	0.00	.16	1	159.7	101
4934.08	Ba II	1	0.00	-.16	1	182.6	98
5853.68	Ba II	2	0.60	-1.01	1	58.1	14
6141.72	Ba II	2	0.70	-.08	1	108.8	38
6496.90	Ba II	2	0.60	-.38	1	88.5	47
3988.52	La II	40	0.40	.05	31	46.9	syn <sup>b</sup>
3995.74	La II	27	0.17	-.03	31	40.0	syn
4086.72	La II	10	0.00	-.18	31	35.7	9
4123.23	La II	41	0.32	-.23	31		syn
4333.32	La II	24	0.17	-.32	31		syn
4073.48	Ce II	4	0.48	.29	31	40.7	syn
4222.60	Ce II	36	0.12	-.19	31	16.0	syn
4460.21	Ce II	2	0.47	.33	31		syn
4062.82	Pr II	2	0.42	.66	31		syn
4143.14	Pr II	4	0.37	.47	31		syn

REFERENCES FOR TABLE 6.—(1) Wiese and Martin 1980. (2) Holweger 1972. (3) Roberts, Anderson and Sorenson 1973a. (4) Kurucz and Peytremann 1975. (5) Allen and Asaad 1957. (6) Smith and Kuhne 1978. (7) Lotrian, Cariou, and Johann-Gilles 1975. (8) Wolnik and Berthel 1973. (9) Whaling, Scalo, and Testerman 1977. (10) Kuhne, Danzmann, and Koch 1978. (11) Bell, Kalman, and Tubbs 1975. (12) Hols and Fuhr 1980. (13) Wolnik *et al.* 1968. (14) Penkin 1964. (15) Bridges and Kornblith 1974. (16) May, Richter, and Wichelmann 1974. (17) Garz and Koch 1969. (18) Bridges and Wiese 1970. (19) Huber and Parkinson 1972. (20) Blackwell *et al.* 1980. (21) Blackwell, Petford, and Shallis 1979. (22) Blackwell *et al.* 1979. (23) Huber and Tubbs 1972. (24) Kurucz 1981. (25) Cardon *et al.* 1982. (26) Huber and Sandemann 1980. (27) Lennard *et al.* 1975. (28) Heise 1974. (29) Hannaford *et al.* 1982. (30) Biemont *et al.* 1981. (31) Anderson *et al.* 1975. (32) Maier and Whaling 1977. (33) Saffman and Whaling 1979. (34) Karner *et al.* 1982. (35) Corliss and Bozman 1962. (36) Smith and Raggett 1981.

Notes: a. The equivalent widths are given in units of mÅ.  
 b. "syn" indicates that this feature was synthesized to derive its abundance.

c. Missing solar equivalent widths indicates either that the line was out of the range of the Liege solar atlas coverage, or that the blending problems were too severe to measure a meaningful line strength.

Roberts, Anderson, and Sorenson (1973*b*). However, Biémont (1978) suggests that these laboratory values are too small and therefore lead to an unacceptably large solar vanadium abundance. Biémont shows that adoption of the semiempirical  $gf$ -values of Kurucz and Peytremann (1975) for this species gives better agreement between solar and meteoritic data for vanadium. Therefore the Kurucz and Peytremann (1975) oscillator strengths are used here.

Cr I, Cr II. Several investigators have reported oscillator strength measurements for Cr I, and most recently Bieniewski (1976) has discussed the scale differences among the published  $gf$  sets. Data are more sparse for Cr II: for most lines we follow Biémont (1978) in employing the Kurucz and Peytremann (1975) semiempirical  $gf$ -values. However, these choices of oscillator strength sets lead to a serious discrepancy between solar chromium abundances derived from neutral and ionized species. From neutral lines Bieniewski (1976) derives  $\log \epsilon(\text{Cr}) = 5.31$ , while Biémont's (1978) ionized line study obtained  $\log \epsilon(\text{Cr}) = 5.88$ . Note that Biémont's (1976) own determination of the solar Cr I abundance, using the Kurucz and Peytremann (1975) semiempirical oscillator strengths, gave  $\log \epsilon(\text{Cr}) = 5.69$ , which is in much better accord with the ionized line result and also with the meteorite data. More experimental work on both species clearly is needed here.

Fe I, Fe II. A large body of experimental data now exists for neutral iron. Extremely reliable  $gf$ -values for Fe I lines with excitation potentials less than 2 eV have been published by Blackwell's Oxford group (see the reference to their series of papers in the table). Their values are adopted without alteration here. For more highly excited Fe I lines the main sources are Bridges and Kornblith (1974) and May, Richter, and Wichelmann (1974). A comparison of their data with those of the Oxford group suggests that there are small systematic differences which are functions of the magnitude of the oscillator strengths (e.g., see the figures in Blackwell, Petford, and Shallis 1979). All scales agree well for large values (greater than  $-1.5$  dex) of  $\log(gf)$ , but the Bridges and Kornblith (1974) and May, Richter, and Wichelmann (1974) scales are higher by about 0.2 dex at small values [about  $\log(gf) = -4$ ]. We have chosen to make a small correction to all data sets other than those of the Oxford group, which linearly increases with progressive weakening of the  $gf$ -value. We recognize that the intercomparisons between Oxford and other investigators has only been possible for low-excitation potential lines, and the discrepancies between the  $gf$  scales may be somewhat less at higher lying levels of Fe I (Blackwell *et al.* 1980). Note here that the problems of  $gf$ -values have been discussed by Huber (1977), and the application of the present set of lab values to stellar spectroscopy previously has been investigated at length by Peterson and Carney (1979). However, most of the

$gf$ -values of the Oxford group, which completely anchor the low excitation potential end of the scale, had not been published by the time of the Peterson and Carney (1979) paper. Also, for high excitation potential Fe I lines we detected in HD 122563 only those whose  $gf$ -values were, typically, greater than  $\log(gf) = -1$ . Such transitions apparently have the most reliably determined oscillator strengths. Therefore, our choices are felt to represent the best which can be achieved at the present time, and we stress the fairly high quality of the overall scale and the large number of determinations of  $gf$ -values of Fe I. Oscillator strengths for Fe II also appear to be fairly well determined. Kurucz (1981) has recently computed semiempirical oscillator strengths for thousands of ionized iron transitions; the figures in his paper show excellent agreement between his work and experimental results.

Co I, Ni I. The new experimental  $gf$ -values of Cardon *et al.* (1982) for Co I were adopted; the solar abundance of cobalt derived by them is in excellent agreement with meteoritic values. For Ni I the oscillator strength scale seems well established, with different investigators producing  $gf$ -values in good agreement with each other.

Y II, Zr II. Recently many workers have turned to oscillator strength work on heavier elements. The papers on yttrium and zirconium by Biémont and collaborators suggest that the good agreement between solar and meteoritic values of these abundances demonstrates the validity of the  $gf$ -value scales.

Ba II. The oscillator strengths given by Wiese and Martin (1980) are essentially identical to those used by Holweger and Müller (1974) for their derivation of the solar Ba abundance.

La II, Ce II, Pr II. The most extensive examination of the oscillator strength scale for rare earths was the lifetime study of Andersen *et al.* (1975). They found shorter lifetimes than those of the Corliss and Bozman (1962)  $gf$ -value compilation, and noted that there was a systematic variation of the lifetime corrections as a function of excitation potential of the upper states of the transitions observed. They concluded, as had others for Fe I, that the most probable source of error in the Corliss and Bozman (1962) lifetimes was an error in the determination of the arc temperature in the earlier experimental setup. However, Andersen *et al.* (1975) felt that since no fault had been found with the intensity measurements of the Corliss-Bozman work, a reasonable procedure was simply to correct the original  $gf$ -values by the ratio of new to old lifetimes. In altering the rare earth  $gf$ -values in this manner, Andersen *et al.* (1975) found much better agreement between solar and meteoritic abundances of nearly all elements. We followed their recommendations explicitly for all lines of La II, as well as for the 4222 Å line of Ce II and the 4143 Å line of Pr II, for which new lifetimes were measured. For other lines of Ce II and Pr II we derived correction

factors for the Corliss-Bozman *gf*-values from the new measured lifetimes for other lines of those species. These correction factors are likely to be fairly reasonable, but contribute an additional uncertainty factor for the abundances of these two elements.

Eu II. A recent series of papers (Meyer *et al.* 1981; Karner *et al.* 1982; Biémont *et al.* 1982) has provided a high-quality set of oscillator strengths for Eu II and a reliable solar Eu abundance. The large hyperfine structure (hfs) splitting of this species has been accounted for in our computations, using the laboratory analysis of the hfs components by Krebs and Winkler (1960). Laboratory hfs data are not available for the 3819 Å and 3907 Å features, but since they are weak in HD 122563 no artificial hfs approximation for these lines was attempted. Two stable isotopes of Eu exist: <sup>151</sup>Eu and <sup>153</sup>Eu. Cameron's (1982) survey of heavy elements in the solar system assigns equal abundance to the two isotopes and suggests that both are made in the *r*-process.

We lacked any clues to the isotopic mix for Eu in HD 122563 and so simply assumed that both isotopes were equally abundant in that star also.

Gd II, Dy II, Er II, Yb II. To our knowledge little laboratory work has been done recently on the *gf*-values for relevant transitions of these species. We are forced to adopt the Corliss and Bozman (1962) *gf*-values here. Note, however, that those same oscillator strengths were used in the derivation of the solar abundances of these rare earth elements by Righini and Rigutti (1966), and Grevesse and Blanquet (1969). Therefore, errors in the relative deficiencies of these elements with respect to the solar contents should be minimized. Moreover, the Grevesse and Blanquet (1969) solar abundances for these four elements are in reasonable agreement with the meteoritic values, and thus the Corliss and Bozman (1962) *gf*-values may be acceptable for the species studied here.

## REFERENCES

- Allen, C. W., and Asaad, A. S. 1957, *M.N.R.A.S.*, **117**, 36.  
 Andersen, T., Poulsen, O., Ramanujam, P. S., and Petrakiev Petkov, A. 1975, *Solar Phys.*, **44**, 257.  
 Bell, R. A., Ericksson, K., Gustafsson, B., and Nordlund, A. 1976, *Astr. Ap. Suppl.*, **23**, 37.  
 Bell, R. A., and Gustafsson, B. 1978, *Astr. Ap. Suppl.*, **34**, 229.  
 Bell, G. D., Kalman, L. B., and Tubbs, E. F. 1975, *Ap. J.*, **200**, 520.  
 Biémont, E. 1976, *Ap. Letters*, **17**, 127.  
 ———. 1978, *M.N.R.A.S.*, **184**, 683.  
 Biémont, E., Grevesse, N., Hannaford, P., and Lowe, R. M. 1981, *Ap. J.*, **248**, 867.  
 Biémont, E., Karner, C., Meyer, G., Trager, F., and zu Putlitz, G. 1982, *Astr. Ap.*, **107**, 166.  
 Bieniewski, T. M. 1976, *Ap. J.*, **208**, 228.  
 Blackwell, D. E., Ibbetson, P. A., Petford, A. D., and Shallis, M. J. 1979, *M.N.R.A.S.*, **186**, 633.  
 Blackwell, D. E., Petford, A. D., and Shallis, M. J. 1979, *M.N.R.A.S.*, **186**, 657.  
 Blackwell, D. E., Petford, A. D., Shallis, M. J., and Simmons, G. J. 1980, *M.N.R.A.S.*, **191**, 445.  
 Bond, H. E. 1980, *Ap. J.*, **44**, 517.  
 Bridges, J. M., and Kornblith, R. L. 1974, *Ap. J.*, **192**, 793.  
 Bridges, J. M., and Wiese, W. L. 1970, *Ap. J.*, **161**, L71.  
 Butcher, H. R. 1972, *Ap. J.*, **176**, 711.  
 ———. 1975, *Ap. J.*, **199**, 710.  
 Cameron, A. G. W. 1982, *Ap. Space Sci.*, **82**, 123.  
 Cardon, B. L., Smith, P. L., Scalo, J. M., Testermann, L., and Whaling, W. 1982, *Ap. J.*, **260**, 395.  
 Cohen, J. G., Frogel, J. A., and Persson, S. E. 1978, *Ap. J.*, **222**, 165.  
 Corliss, C. H., and Bozman, W. R. 1962, *NBS Monog.*, No. 53.  
 Corliss, C. H., and Tech, J. L. 1968, *NBS Monog.*, No. 108.  
 Couch, R. G., Schmiedekamp, A. B., and Arnett, W. D. 1974, *Ap. J.*, **190**, 95.  
 Cowan, J. J., Cameron, A. G. W., and Truran, J. W. 1980, *Ap. J.*, **241**, 1090.  
 ———. 1982, *Ap. J.*, **252**, 348.  
 Cowley, C. R., and Downs, P. L. 1980, *Ap. J.*, **236**, 648.  
 Delbouille, L., Neven, L., and Roland, G. 1973, *Photometric Atlas of the Solar Spectrum from  $\lambda$ 3000 to  $\lambda$ 10,000* (Liège: Institut d'Astrophysique).  
 Garz, T., and Koch, M. 1969, *Astr. Ap.*, **2**, 274.  
 Grevesse, N., and Blanquet, G. 1969, *Solar Phys.*, **8**, 5.  
 Griffin, R., Griffin, R., Gustafsson, B., and Vieira, T. 1982, *M.N.R.A.S.*, **198**, 637.  
 Gustafsson, B., Bell, R. A., Fredga, K., and Gahm, G. F. 1980, *Astr. Ap.*, **89**, 255.  
 Hannaford, P., Lowe, R. M., Grevesse, N., Biémont, E., and Whaling, W. 1982, *Ap. J.*, **261**, 736.  
 Heise, H. 1974, *Astr. Ap.*, **34**, 275.  
 Hinkle, K. H., and Lambert, D. L. 1975, *M.N.R.A.S.*, **170**, 447.  
 Holweger, H. 1971, *Astr. Ap.*, **12**, 319.  
 ———. 1972, *Solar Phys.*, **25**, 14.  
 Holweger, H., and Müller, E. A. 1974, *Solar Phys.*, **39**, 19.  
 Holys, A., and Fuhr, J. R., 1980, *Astr. Ap.*, **90**, 14.  
 Huber, M. C. E. 1977, *Phys. Scripta*, **16**, 16.  
 Huber, M. C. E., and Parkinson, W. H. 1972, *Ap. J.*, **172**, 229.  
 Huber, M. C. E., and Sandemann, R. J. 1980, *Astr. Ap.*, **86**, 95.  
 Huber, M. C. E., and Tubbs, E. F. 1972, *Ap. J.*, **177**, 847.  
 Johnson, H. L. 1966, *Ann. Rev. Astr. Ap.*, **4**, 193.  
 Karner, C., Meyer, G., Trager, F., and zu Putlitz, G. 1982, *Astr. Ap.*, **107**, 161.  
 Koelbloed, D. 1967, *Ap. J.*, **149**, 299.  
 Krebs, K., and Winkler, R. 1960, *Zs. Phys.*, **160**, 320.  
 Kuhne, M., Danzmann, K., and Koch, M. 1978, *Astr. Ap.*, **64**, 111.  
 Kurucz, R. L. 1970, *SAO Spec. Rpt.*, No. 309.  
 ———. 1981, *SAO Spec. Rpt.*, No. 390.  
 Kurucz, R. L., and Peytremann, E. 1975, *SAO Spec. Rpt.*, No. 362.  
 Lamb, S. A., Howard, W. M., Truran, J. W., and Iben, I., Jr. 1977, *Ap. J.*, **217**, 213.  
 Lambert, D. L. 1978, *M.N.R.A.S.*, **182**, 249.  
 Lambert, D. L., and Luck, R. E. 1978, *M.N.R.A.S.*, **183**, 79.  
 Lambert, D. L., and Ries, L. M. 1981, *Ap. J.*, **217**, 508.  
 Lambert, D. L., and Sneden, C. 1977, *Ap. J.*, **215**, 597.  
 Lambert, D. L., Sneden, C., and Ries, L. M. 1974, *Ap. J.*, **188**, 97.  
 Lennard, W. N., Whaling, W., Scalo, J. M., and Testerman, L. 1975, *Ap. J.*, **197**, 517.  
 Lotrian, J., Cariou, J., and Johannin-Gilles, A. 1975, *J. Quant. Spectrosc. Rad. Transf.*, **15**, 815.  
 Luck, R. E., and Bond, H. E. 1981, *Ap. J.*, **244**, 919.  
 Mackle, R., Holweger, H., Griffin, R., and Griffin, R. 1975, *Astr. Ap.*, **38**, 239.  
 Maier, R. S., and Whaling, W. 1977, *J. Quant. Spectrosc. Rad. Transf.*, **18**, 501.  
 May, M., Richter, J., and Wichelmann, J. 1974, *Astr. Ap. Suppl.*, **18**, 405.  
 Meggers, W. F., Corliss, C. H., and Scribner, B. F. 1975, *NBS Monog.*, No. 145.  
 Meyer, G., Ruland, W., Sahn, A., and zu Putlitz, G. 1981, *Astr. Ap.*, **95**, 278.  
 Minnaert, M., Mulders, G. F. W., and Houtgast, J. 1940, *Photometric Atlas of the Solar Spectrum* (Amsterdam: D. Schnabel).  
 Moore, C. E., Minnaert, M. G. J., and Houtgast, J. 1966, *The Solar Spectrum 2935 Å to 8770 Å*, *NBS Monograph 61*.

- Pagel, B. E. J. 1964, *Roy. Obs. Bull.*, No. 87.  
 ———. 1965, *Roy. Obs. Bull.*, No. 104.
- Penkin, N. P. 1964, *J. Quant. Spectrosc. Rad. Transf.*, **4**, 85.
- Peterson, R. C. 1976, *Ap. J.*, **206**, 800.
- Peterson, R. C., and Carney, B. W. 1979, *Ap. J.*, **231**, 762.
- Ries, L. M. 1982, Ph.D. thesis, University of Texas, Austin.
- Righini, A., and Rigutti, M. 1966, *Ann. d'Ap.*, **29**, 379.
- Roberts, J. R., Anderson, T., and Sorensen, G. 1973*a*, *Ap. J.*, **181**, 567.  
 ———. 1973*b*, *Ap. J.*, **181**, 587.
- Ross, J. E., and Aller, L. H. 1976, *Science.*, **191**, 1223.
- Ruland, F., Holweger, H., Griffin, R., Griffin, R., and Biehl, D. 1980, *Astr. Ap.*, **92**, 70.
- Sackmann, I.-J., Smith, R. L., and Despaigne, K. H. 1974, *Ap. J.*, **187**, 555.
- Saffman, L., and Whaling, W. 1979, *J. Quant. Spectrosc. Rad. Transf.*, **21**, 93.
- Smith, G. 1981, *Astr. Ap.*, **103**, 351.
- Smith, P. L., and Kuhne, M. 1978, *Proc. Roy. Soc. London, A*, **362**, 263.
- Smith, G., and Raggett, D. St. J. 1981, *J. Phys. B: Atom. Molec. Phys.*, **14**, 4015.
- Sneden, C. 1973, *Ap. J.*, **184**, 839.
- Sneden, C., Lambert, D. L., and Pilachowski, C. A. 1981, *Ap. J.*, **247**, 1052.
- Spite, M., and Spite, F. 1979, *Astr. Ap.*, **76**, 150.
- Tomkin, J. 1972, *M.N.R.A.S.*, **156**, 349.
- Tomkin, J., and Lambert, D. L. 1982, preprint.
- Trimble, V. 1975, *Rev. Mod. Phys.*, **47**, 877.
- Truran, J. W. 1981*a*, *Astr. Ap.*, **97**, 391.  
 ———. 1981*b*, in *Progress in Particle and Nuclear Physics* (Oxford: Pergamon Press), p. 161.
- Truran, J. W., and Iben, I., Jr. 1977, *Ap. J.*, **216**, 797.
- Tull, R. G., Choisser, J. P., and Snow, E. H. 1975, *Appl. Opt.*, **14**, 1182.
- Vogt, S. S., Tull, R. G., and Kelton, P. 1978, *Appl. Opt.*, **17**, 574.
- Wallerstein, G., Greenstein, J. L., Parker, R., Helfer, H. L., and Aller, L. H. 1963, *Ap. J.*, **137**, 280.
- Whaling, W., Scalo, J. M., and Testerman, L. 1977, *Ap. J.*, **212**, 581.
- Wiese, W. L., and Martin, G. A. 1980, *NSRDS-NBS*, No. 68.
- Wolff, S. C., and Wallerstein, G. 1967, *Ap. J.*, **150**, 257.
- Wolfram, W. 1977, *Ap. J.*, **17**, 17.
- Wolnik, S. J., and Berthel, R. O. 1973, *Ap. J.*, **179**, 665.
- Wolnik, S. J., Berthel, R. O., Larson, G. S., Carnevale, E. H., and Wares, G. W. 1968, *Phys. Fluids*, **11**, 1002.

M. PARTHASARATHY and CHRISTOPHER SNEDEN: Department of Astronomy, 15.220 R. L. Moore Hall, University of Texas at Austin, Austin, TX 78712